fermentation

MDPI

Article

Growth Prediction and Metabolite Profiling of Probiotic *Lactobacilli* Cultivated with Eggshell Membrane Protein: A Comparison of Kinetic Models and Machine Learning Methods

Tulay Ozcan [1,*], Lutfiye Yilmaz-Ersan [1], Gokce Keser [1], Merve Begum Narli [2] and Murat Olcay Ozcan [3]

[1] Department of Food Engineering, Faculty of Agriculture, Bursa Uludag University, Bursa 16059, Türkiye; lutfiyey@uludag.edu.tr (L.Y.-E.); gokcekeser@uludag.edu.tr (G.K.)
[2] Department of Food Processing, Susurluk Vocational School of Agriculture and Forestry, Balikesir University, Balikesir 10600, Türkiye; begum.narli@balikesir.edu.tr
[3] Department of Software Engineering, Faculty of Engineering, Kirklareli University, Kirklareli 39100, Türkiye; moozcan@klu.edu.tr
* Correspondence: tulayozcan@uludag.edu.tr

Abstract

This study addressed two main scientific questions: whether eggshell membrane (ESM) protein influences probiotic growth and metabolite production in a strain-dependent manner, and which predictive modeling approach provides the most accurate estimation of bacterial growth. This study aimed to determine the effects of ESM protein on the growth kinetics and metabolite profiles of *Lactobacillus acidophilus*, *Lacticaseibacillus paracasei* subsp. *casei*, and *Lacticaseibacillus rhamnosus* strains, and to compare the performance of various predictive models. Microbial growth, pH, and metabolite profiles were evaluated during 24 h of fermentation in control and ESM-containing media. Growth data were modeled using the modified Gompertz, Baranyi–Roberts, Gaussian process regression (GPR), and support vector regression (SVR) methods, with validation performed by withholding one intermediate time point at a time within each growth curve. The impact of ESM on growth kinetics was found to be strain-dependent; according to the modified Gompertz model, the maximum specific growth rate of *L. casei* increased from 0.53 to 0.73 h^{-1}, whereas those of *L. acidophilus* and *L. rhamnosus* decreased from 0.94 to 0.47 h^{-1} and from 0.72 to 0.56 h^{-1}, respectively. GPR yielded the lowest mean cross-validated root mean squared error (CV_RMSE = 0.1344 $\log_{10}$ CFU/mL), followed by SVR (0.1359), Baranyi–Roberts (0.1533), and modified Gompertz (0.1657), although the best-performing method varied among conditions. Significant changes in amino acid profiles were observed in media containing ESM, with total amino acid content increasing, particularly in the *L. acidophilus* group, from 344.90 to 2773.70 mg/kg after 24 h of fermentation. Lactic acid and SCFAs were also influenced by both the microorganism and the culture medium composition, with the highest final lactic acid concentration (3082.88 mg/kg) observed in the control *L. rhamnosus* medium. The findings indicate that ESM can be considered an alternative medium component in strain-specific fermentation processes, and that the choice of model should be based on the experimental conditions and cross-validated predictive performance.

Keywords: eggshell membrane protein; probiotic *lactobacilli*; growth kinetics; predictive microbiology; machine learning; metabolites

Check for updates

Academic Editor: Peng Wu

Received: 23 October 2026
Revised: 10 November 2026
Accepted: 12 November 2026
Published: 15 November 2026

Copyright: © 2026 by the authors. Licensee MDPI, Basel, Switzerland. This article is an open access article distributed under the terms and conditions of the Creative Commons Attribution (CC BY) license.

1. Introduction

Eggs are among the most widely consumed foods today due to their high-quality, balanced nutritional content, accessibility, and low cost [1]. The global increase in egg production also leads to a rise in egg waste; typically discarded, this waste can result in potential revenue loss, environmental pollution, and health issues. Therefore, it is crucial to conduct research to improve waste management, alleviate ecological burdens, and transform these products into valuable assets through biological, environmental, and agricultural engineering applications, thereby enhancing their potential for use in the food sector [2–4].

Eggs have a relatively low carbon footprint among animal-based foods; however, production processes still result in high emissions that can be linked to environmental impacts. To reduce greenhouse gas emissions associated with egg production, it is recommended to promote the use of alternative sources and increase the value-added potential of by-products to offset emissions generated during primary production [5,6].

The rapid development of agriculture and industry is increasing the volume of agricultural products consumed, resulting in more by-products and biological waste. Similarly, the rapid development of the modern egg industry leads to the generation of numerous egg by-products, such as eggshells (ESs), eggshell membranes (ESMs), salted egg white, and defatted egg yolk proteins, that possess various functional properties and biological activities but are not effectively utilized [7]. ESM, a nanofibrous material derived from egg by-products, is a low-cost bioresource with high biological activity. There is potential to use this component to develop next-generation, eco-friendly solutions that contribute to the circular economy by enabling recycling. Recently, developing new functional products from recycled biological waste has become of great importance for sustainable environmental policies [8].

ESM is mainly generated as a by-product of industrial egg-breaking and egg-processing operations, where the eggshell and its associated membrane remain after the removal of liquid egg contents. Eggshells account for approximately 10–12% of the total egg weight, while ESM represents approximately 1.02%. Based on global egg production in 2020, the potential annual generation of ESM has been estimated at approximately 883,800 tonnes, indicating its substantial availability as an underutilized bioresource. ESM can be recovered from collected eggshell residues through physical, chemical, or enzymatic separation methods. Physical approaches generally involve washing, drying, crushing, and separating the membrane from the mineralized shell using differences in particle density and mechanical properties, whereas chemical and enzymatic methods facilitate membrane detachment through selective treatment. The recovery and valorization of ESM from egg-processing residues may therefore provide an opportunity to reduce waste while developing alternative nutrient sources for microbial fermentation [9].

A common food by-product, ESM, is a membrane approximately 100 μm thick that lies between the egg white and the hard eggshell and is composed of calcium and phosphate. It is rich in protein, comprising about 90% protein, including 10% collagen types I, V, and X, and contains glycoproteins and lysine-derived cross-links. Additionally, its structure includes polysaccharides such as hyaluronic acid and chondroitin sulfate [2,4,8]. Eggshell membrane is an ingredient that can be incorporated into nutritional supplements due to its synergistic effects. Some studies have indicated that it may exert anti-obesity effects by regulating the gut microbiota, enriching the diversity within the gut, and supporting lipid metabolism [10]. Furthermore, given its high content of fibrous proteins and moderate amounts of collagen, hyaluronic acid, chondroitin sulfate, and glucosamine, it is believed to exert physiological effects similar to those of dietary fiber [11].

Lactic acid and probiotic fermentation are eco-friendly, 'green' technologies through which lactic acid bacteria (LAB) contribute to waste management by recovering valuable biomolecules from waste materials [12]. It is known that lactic acid bacteria possess prote-

olytic systems consisting of cell-membrane proteinases and intracellular peptides. Therefore, it was thought that the selected bacteria would catalyze the breakdown of proteins into oligopeptides during fermentation and could positively influence the degradation of egg-derived low-molecular-weight peptides and amino acids via intracellular peptidases.

Fermentation is significantly influenced by optimizing factors that affect microbial growth. These factors shape the specific conditions of each microorganism's environment, thereby impacting fermentation kinetics. The fermentation kinetics of lactic acid bacteria (LAB), which play a crucial role in fermented foods, provide insights into the rate of cellular biomass production and growth [13,14]. Modeling microbial growth is one of the primary objectives of predictive microbiology. The growth of a bacterial culture is characterized by four distinct phases: the lag phase, the exponential (logarithmic) phase, the stationary phase, and the death phase. In recent years, various mathematical models have been developed to predict microbial growth, providing quantitative estimates of changes in bacterial populations under specific experimental conditions. In the literature, several predictive models—such as the logistic, Baranyi–Roberts, modified Gompertz, and Huang models—are employed to describe bacterial growth as a function of time [15]. These mathematical models contribute to a better understanding of the fermentation process and facilitate the development of optimization techniques to ensure its economic viability. The purpose of these models is to mathematically relate biochemical characteristics (response variables) to environmental conditions, such as temperature, pH, water activity, and substrate composition (control variables). This approach helps to improve the management of the fermentation process [16,17].

Kernel-based regression methods provide an alternative for describing growth trajectories without specifying a sigmoidal equation. Gaussian process regression (GPR) has been applied to microbial growth curves to estimate growth dynamics and quantify uncertainty in interpolated values [18]. Support vector regression (SVR) provides a regularized approach to nonlinear function estimation, balancing model complexity against deviations from the observed values [19]. These methods can therefore be evaluated alongside primary growth models to examine whether their flexibility improves the estimation of cell densities at unobserved intermediate times. For this purpose, agreement with the observations used for fitting should be distinguished from performance at time points withheld during model development.

Although alternative substrates and mathematical models have been widely investigated in microbial fermentation, their combined evaluation in the context of ESM-based culture media remains limited. The novelty of this study lies in the integrated assessment of strain-dependent growth kinetics and metabolite profiles in ESM-containing media, together with a systematic comparison of conventional kinetic models (modified Gompertz and Baranyi–Roberts) and machine learning methods (GPR and SVR). Unlike studies focusing solely on substrate utilization or growth modeling, the present work evaluates both biological responses and predictive performance within a common experimental framework. Furthermore, the inclusion of cross-validation at withheld intermediate time points provides additional insight into the interpolation capabilities of these modeling approaches.

The main hypothesis of this study was that replacing conventional nitrogen sources with ESM-containing material would alter the growth kinetics and metabolite profiles of probiotic lactobacilli in a strain-dependent manner. Accordingly, the primary objective was to investigate the growth kinetics, pH changes, and metabolite profiles of *Lactobacillus acidophilus*, *Lacticaseibacillus paracasei* subsp. *casei*, and *Lacticaseibacillus rhamnosus* in ESM-containing culture media, while a complementary objective was to compare the predictive performance of conventional kinetic models and machine learning methods. For this purpose, the modified Gompertz and Baranyi–Roberts models were compared with

Gaussian process regression (GPR) and support vector regression (SVR) to estimate $\log_{10}$ cell densities as a function of fermentation time. The kinetic and machine learning models were applied independently to the same experimental datasets rather than integrated into a hybrid model. Model performance was evaluated based on both goodness of fit and predictions at withheld intermediate time points, using linear interpolation as a reference. This comparative approach provides insights into strain-specific fermentation responses and the selection of suitable predictive methods, while supporting the potential valorization of ESM as an alternative medium component within a circular economy framework.

2. Materials and Methods

2.1. Materials and Reagents

Eggshell membrane powder (80% protein) was obtained from Egglin Food (Bandirma, Balikesir, Türkiye). Its compositional characteristics are presented in Table 1. The ESM powder was obtained as a commercially processed ingredient, and no additional eggshell membrane collection or separation procedures were performed in the present study. The *Lactobacillus acidophilus* (Nu-trish® LA-5®), *Lacticaseibacillus paracasei* subsp. *casei* (Nu-trish® *L. casei* 431®), and *Lacticaseibacillus rhamnosus* (Nu-trish® LGG®) cultures used in the study were obtained from Novonesis/Chr. Hansen (Hørsholm, Denmark). The following components were used to prepare the culture medium; peptone (Merck, Darmstadt, Germany), yeast extract (Biolife, Milan, Italy), meat extract (Biolife, Milan, Italy), glucose (Sigma-Aldrich, Taufkirchen, Germany), sodium acetate (CH_3COONa) (Merck, Darmstadt, Germany), Tween 80 (Merck, Darmstadt, Germany), dipotassium phosphate (K_2HPO_4) (Merck, Darmstadt, Germany), ammonium citrate ($(NH_4)_3C_6H_5O_7$) (Merck, Darmstadt, Germany), magnesium sulfate ($MgSO_4 \cdot 7H_2O$) (Merck, Darmstadt, Germany), and manganese sulfate ($MnSO_4 \cdot H_2O$) (Merck, Darmstadt, Germany).

Table 1. Composition and characteristics of eggshell membrane powder.

Property	Specification
Physical properties	
Taste	Neutral
Odor	Characteristic odor
Color	Unique, pinkish-white powder
Structure	200–350 µm powder
Chemical properties	
Protein	Minimum 80%
Collagen (types I, V, and X)	Minimum 10%
Elastin	Minimum 15%
Total glycosaminoglycans (GAGs)	Minimum 4%
Hyaluronic acid	Minimum 2%
Moisture (% *w*/*w*)	Maximum 5%
Heavy metals (Hg, As, Pd, Cd)	<1 mg/kg
Microbiological properties	
Salmonella	Absent in 25 g
Enterobacteriaceae (CFU/g)	<10
Aerobic colonies (CFU/g)	Maximum 10^2

2.2. Methods

2.2.1. Activation of Bacterial Cultures

Lyophilized cultures of *L. acidophilus*, *L. casei*, and *L. rhamnosus* were each added separately to 25 mL of sterile de Man, Rogosa, and Sharpe (MRS) broth (Merck, Germany)

at a concentration of 1% (*w*/*v*; 0.25 g of lyophilized culture per 25 mL of broth) and incubated at 37 °C for 24 h. The tubes containing active cells were centrifuged at 6000× *g* for 20 min at 4 °C; the supernatant was then removed, and the cells were washed with sterile distilled water. The resulting pellets were inoculated into the culture media to achieve a concentration of approximately 10^7–10^8 colony-forming units per milliliter (CFU/mL) [20].

2.2.2. Preparation of MRS Broth Media and Experimental Design

The compositions of the culture media are presented in Table 2. The culture media were designed to evaluate the suitability of ESM as an alternative to conventional complex nitrogen sources in MRS broth. In the ESM-containing media, peptone (10 g/L), yeast extract (5 g/L), and meat extract (10 g/L) were replaced with ESM powder at a concentration of 25 g/L, corresponding to a mass-based replacement of the conventional complex nitrogen sources. Glucose, salts, and other medium components were maintained at the same concentrations as in the control media. This formulation allowed the growth responses of the selected probiotic strains to be compared under different nitrogen-source conditions. However, because ESM contains structurally complex proteins, its nitrogen availability may differ from that of the readily accessible peptides, amino acids, and other nutrients supplied by conventional MRS components. Therefore, differences in microbial growth and metabolite production were expected to depend on the nutritional requirements and substrate utilization capacities of the individual bacterial strains. The prepared media were heat-treated at 90 °C for 10 min. Once cooled to 37 ± 1 °C, the media were inoculated with 3% (*v*/*v*) of the activated bacterial culture suspension and incubated at 37 °C. For each bacterial strain and culture medium condition, two independent fermentation batches were prepared as biological replicates. Analytical measurements were performed in triplicate for each fermentation batch, except for bacterial enumeration used in growth modeling, for which one count from each independent fermentation batch was used. Results are presented as mean ± standard deviation (SD).

Table 2. Composition of the culture medium.

	CLA	CLC	CLR	ELA	ELC	ELR
Peptone (10 g/L)	X	X	X			
Yeast extract (5 g/L)	X	X	X			
Meat extract (10 g/L)	X	X	X			
Glucose (20 g/L)	X	X	X	X	X	X
Sodium acetate (CH_3COONa) (5 g/L)	X	X	X	X	X	X
Tween 80 (1 mL/L)	X	X	X	X	X	X
Dipotassium phosphate (K_2HPO_4) (2 g/L)	X	X	X	X	X	X
Ammonium citrate ($(NH_4)_3C_6H_5O_7$) (2 g/L)	X	X	X	X	X	X
Magnesium sulfate ($MgSO_4 \cdot 7H_2O$) (0.2 g/L)	X	X	X	X	X	X
Manganese sulfate ($MnSO_4 \cdot H_2O$) (0.05 g/L)	X	X	X	X	X	X
Eggshell membrane (25 g/L)				X	X	X
L. acidophilus	X			X		
L. casei		X			X	
L. rhamnosus			X			X

Note: CLA: culture medium containing *L. acidophilus*; CLC: culture medium containing *L. casei*; CLR: culture medium containing *L. rhamnosus*; ELA: culture medium containing eggshell membrane protein and *L. acidophilus*; ELC: culture medium containing eggshell membrane protein and *L. casei*; ELR: culture medium containing eggshell membrane protein and *L. rhamnosus*.

2.2.3. Bacteria Counts

LAB counts were evaluated using MRS agar under anaerobic conditions at 37 °C for 72 h. These counts were performed on medium samples at storage intervals of 0, 3, 6, 9, 12,

15, 18, 21, and 24 h. Colony counts were expressed as logarithmic values ($\log_{10}$ CFU/mL) following the methodology of [21].

2.2.4. pH

The pH of the samples was determined using a portable pH meter (pH 3110 Set 2; WTW, Weilheim, Germany). Prior to each measurement, the instrument was calibrated with standard buffer solutions of pH 4.0 and 7.0 at 20 °C. Changes in pH were monitored at 3-h intervals over a 24-h period [22].

2.2.5. Kinetic Modeling and Preparation of Growth Data

Cell counts in the CLA, CLC, CLR, ELA, ELC, and ELR samples were determined at 3-h intervals over 24 h, yielding nine time points, including the initial measurement. For each culture condition and sampling time, bacterial counts were obtained from two independent fermentation batches. The counts were converted to $\log_{10}$ CFU/mL, and the arithmetic mean of the two logarithmic values was used as the observed response for growth modeling. Thus, each growth model was fitted to one mean $\log_{10}$ CFU/mL value per sampling time, rather than treating the two biological replicates as separate observations. Owing to declines in the final phase, measurements at 21 and 24 h for CLA and CLC and at 24 h for CLR and ELC were excluded from growth model fitting, whereas all measurements for ELA and ELR were retained.

For cell counts N (CFU/mL) and logarithmic cell density y, the model input was calculated using Equation (1):

$$y_{ij} = log_{10}\left(N_{ij}\right), \qquad \overline{y}_i = \frac{1}{2}\sum_{j=1}^{m} y_{ij} \tag{1}$$

Here, i denotes the time point, j denotes the parallel measurement, and m is the number of parallel measurements. The SD of the parallel logarithmic measurements was calculated as the sample standard deviation using Equation (2):

$$SD_i = \sqrt{\frac{\sum_{j=1}^{m}\left(y_{ij} - \overline{y}_i\right)^2}{m-1}} \tag{2}$$

Growth curves were fitted using the modified Gompertz model described by [23], expressed on the $\log_{10}$ scale, as shown in Equation (3):

$$\hat{y}(t) = y_0 + A\exp\left[-\exp\left\{\frac{r_{max}e}{A}(\lambda - t) + 1\right\}\right] \tag{3}$$

Here, t is time (h), $\hat{y}(t)$ is the predicted cell counts in $\log_{10}$ CFU/mL, y_0 is the lower asymptote, A is the asymptotic logarithmic increase, r_{max} is the maximum slope ($\log_{10}$ CFU/mL h^{-1}), λ is the lag time (h), and e is Euler's number. The upper asymptote was calculated using Equation (4):

$$y_{max} = y_0 + A \tag{4}$$

The maximum specific growth rate on the natural logarithmic scale, μ_{max} (h^{-1}), was obtained using the following conversion Equation (5):

$$\mu_{max} = \ln(10)\, r_{max} \tag{5}$$

The initial model prediction was calculated separately from the lower asymptote Equation (6):

$$\hat{y}(0) = y_0 + A\exp\left[-\exp\left\{\frac{r_{max}e\lambda}{A} + 1\right\}\right] \tag{6}$$

The four-parameter form of the Baranyi–Roberts model [24] was used, with the shape parameter for population limitation set to 1 and the adaptation rate set to μ_{max}. The adaptation-adjusted time function $F(t)$ and the predicted cell counts on the $\log_{10}$ scale were expressed using Equations (7)–(9):

$$h_0 = \mu_{max}\lambda \tag{7}$$

$$F(t) = t + \frac{1}{\mu_{max}} \ln[\exp(-\mu_{max}t) + \exp(-h_0) - \exp(-\mu_{max}t - h_0)] \tag{8}$$

$$\hat{y}(t) = y_0 + \frac{\mu_{max}F(t)}{\ln(10)} - \frac{1}{\ln(10)} \ln\left[1 + \frac{\exp\{\mu_{max}F(t)\} - 1}{\exp\{(y_{max} - y_0)\ln(10)\}}\right] \tag{9}$$

Here, y_0 is the initial logarithmic cell counts, y_{max} is the upper asymptote, and h_0 is the dimensionless initial adaptation parameter. The units of μ_{max} are h^{-1}, whereas λ and $F(t)$ are expressed in hours. For the Baranyi model, $F(0) = 0$ and $\hat{y}(0) = y_0$.

Parameters for both models were estimated by unweighted nonlinear least squares using the same included time points. The transformations $A = y_{max} - y_0$ and $r_{max} = \mu_{max}/\ln(10)$ were used to jointly estimate four free parameters (Equation (10)):

$$\theta^* = \underset{\theta}{\operatorname{argmin}} \sum_{i=1}^{n} \left[\overline{y}_i - \hat{y}(t_i;\theta)\right]^2, \qquad \theta = (y_0, A, r_{max}, \lambda) \tag{10}$$

Parameter estimation was performed using the least-squares function.

The doubling time g (h), asymptotic number of generations, G_∞, and generation rate were calculated using the following equations (Equations (11) and (12)):

$$g = \frac{\ln(2)}{\mu_{max}} = \frac{\log_{10}(2)}{r_{max}}, \qquad G_\infty = \frac{A}{\log_{10}(2)} \tag{11}$$

$$\text{Generation rate} = \frac{1}{g} = \frac{\mu_{max}}{\ln(2)} \tag{12}$$

2.2.6. Machine Learning Models

Gaussian process regression (GPR) and support vector regression (SVR) were used to estimate $\log_{10}$ cell counts as a function of fermentation time. A separate model was fitted for each of the six culture conditions. The recorded mean $\log_{10}$ CFU/mL values were used without further rounding, and the time points included in the analysis were the same as those used for the modified Gompertz and Baranyi–Roberts models. Fermentation time, divided by 24 h, was the sole predictor; pH and metabolite measurements were not included as model inputs. The four models were fitted independently; kinetic parameters or predictions were not used as inputs to GPR or SVR. The dataset comprised 54 condition–time records, of which 48 were retained for modelling; each model used only the seven to nine observations belonging to its culture condition.

GPR was implemented using a Matérn covariance function with a smoothness parameter of $\nu = 2.5$, multiplied by a constant covariance amplitude and combined with an additive white-noise term. Gaussian process methods have previously been used to analyse microbial growth curves and estimate uncertainty in interpolated values [18]. The response was standardized using the mean and standard deviation of the training observations, and predictions were transformed back to the original $\log_{10}$ scale. Kernel parameters were estimated by maximizing the log marginal likelihood, with two additional optimizer restarts. The initial covariance amplitude, length scale, and noise level were 1.0, 0.25, and 0.01, respectively; their optimization bounds were 10^{-3}–10^2, 0.03–3.0, and 10^{-5}–0.3. A diagonal term of 10^{-8} was added for numerical stability.

SVR was implemented with a radial basis function kernel [19]. The regularization parameter C, the ε-insensitive loss parameter, and the kernel coefficient γ were selected from $C \in \{1, 10, 100\}$, $\varepsilon \in \{0.01, 0.05, 0.10\}$, and $\gamma \in \{1, 10\}$, respectively. Parameter combinations were evaluated by an inner cross-validation procedure in which intermediate training time points were withheld one at a time while the first and last training points were retained. The combination with the lowest mean squared prediction error was selected. The response values were not standardized for SVR.

The machine learning models were implemented in Python using scikit-learn version 1.9.1 [25]. A fixed random seed was used for GPR optimization.

2.2.7. Goodness-of-Fit Assessment

Model fit was evaluated using the sum of squared errors (SSE), root mean squared error (RMSE), and coefficient of determination (R^2) (Equations (13)–(15)):

$$SSE = \sum_{i=1}^{n} (\overline{y}_i - \hat{y}_i)^2 \tag{13}$$

$$RMSE = \sqrt{\frac{SSE}{n}} \tag{14}$$

$$R^2 = 1 - \frac{\sum_{i=1}^{n} (\overline{y}_i - \hat{y}_i)^2}{\sum_{i=1}^{n} (\overline{y}_i - \overline{y})^2}, \qquad \overline{y} = \frac{1}{n} \sum_{i=1}^{n} \overline{y}_i \tag{15}$$

Here, $\overline{y}_i$ is the observed mean logarithmic cell counts, $\hat{y}_i$ is the model prediction, $\overline{y}$ is the overall mean of the observations included in the fit, and n is the number of included time points. The values of n were 7 for CLA and CLC, 8 for CLR and ELC, and 9 for ELA and ELR. RMSE was expressed in $\log_{10}$ CFU/mL and calculated using n as the denominator. The modified Gompertz, Baranyi–Roberts, GPR, and SVR models were evaluated using the same included observations for each culture condition. Lower SSE and RMSE values and higher R^2 values indicated closer agreement with the observations used for fitting. These measures described in-sample fit and were reported separately from the prediction errors obtained by withholding intermediate time points.

2.2.8. Validation at Withheld Intermediate Time Points

Prediction performance was assessed separately for each culture condition by withholding one intermediate time point at a time. The first and last included observations were retained in every training set to evaluate interpolation within the observed time range. This validation design is consistent with the use of leave-one-out cross-validation to assess interpolation performance within an observed time series [26]. This procedure yielded five withheld predictions for CLA and CLC, six for CLR and ELC, and seven for ELA and ELR. Measurements excluded from growth model fitting were also excluded from this validation procedure. No fixed random training–test split was used. At each outer validation step, one intermediate observation was withheld, and the model was fitted to the remaining observations. The training-to-validation counts were therefore 6:1 for CLA and CLC, 7:1 for CLR and ELC, and 8:1 for ELA and ELR, corresponding to 85.7%:14.3%, 87.5%:12.5% and 88.9%:11.1%, respectively.

The modified Gompertz, Baranyi–Roberts, GPR and SVR models were refitted to the remaining observations at each validation step. For GPR, response standardization and kernel parameter estimation were performed using only the training observations. For SVR, the parameter search was repeated within each training set using the inner validation procedure described above. The withheld response value was not used for model fitting or parameter selection. Linear interpolation between the nearest remaining observations on either side of the withheld time point was included as a reference method.

For each model and culture condition, predictions from all withheld intermediate time points were combined to calculate the cross-validated root mean squared error (CV_RMSE), mean absolute error (CV_MAE) and coefficient of determination (CV_R^2) (Equations (16)–(18)):

$$\text{CV_RMSE} = \sqrt{\frac{\sum_{i=1}^{n_H}\left(y_i - \hat{y}_{i,-i}\right)^2}{n_H}} \quad (16)$$

$$\text{CV_MAE} = \frac{\sum_{i=1}^{n_H}\left|y_i - \hat{y}_{i,-i}\right|}{n_H} \quad (17)$$

$$\text{CV_R}^2 = 1 - \frac{\sum_{i=1}^{n_H}\left(y_i - \hat{y}_{i,-i}\right)^2}{\sum_{i=1}^{n_H}\left(y_i - \bar{y}_H\right)^2} \quad (18)$$

Here, n_H is the number of withheld intermediate time points, y_i is the observed $\log_{10}$ cell counts, $\hat{y}_{i,-i}$ is its prediction from a model fitted without that observation, and $\bar{y}_H$ is the mean of the observed values at the withheld time points. CV_RMSE and CV_MAE were expressed in $\log_{10}$ CFU/mL. CV_R^2 was calculated from the combined withheld predictions rather than separately for each validation step.

Results were reported for each culture condition and summarized as the unweighted arithmetic mean of the six condition-specific scores. Each condition therefore contributed equally to the overall comparison, irrespective of the number of observations included. Model comparisons were descriptive; no statistical significance tests were applied to differences between validation scores. The validation assessed interpolation within the selected portion of each growth curve. Because the growth-phase exclusions were fixed before validation, the results were conditional on this selection. They did not assess forecasting beyond the observed time range or predictive performance in independent fermentation experiments. Thus, the predictive analysis was limited to describing the observed experimental growth trajectories and estimating cell densities at withheld intermediate time points within the same culture conditions. The models were not developed or validated to predict microbial growth under different temperatures, initial pH values, ESM concentrations, or other untested fermentation conditions. After validation, each model was fitted to all included observations for the presentation of the final growth curves and in-sample fit statistics.

2.2.9. Amino Acid Analysis

The amino acid analysis performed at 0 h and 24 h of the fermentation period followed the method described by [27]. High-performance liquid chromatography (HPLC) (Shimadzu Prominence, Kyoto, Japan) equipped with a diode array detector (DAD, SPD-M20A) and an autosampler (SIL 20ACHT) was used for the analysis. A mobile phase gradient of 0.1 M ammonium acetate and acetonitrile was used at a flow rate of 1 mL/min. Samples were separated using an ACE5 C-18 column (250 × 4.6 mm, 5 µm) maintained at 40 °C. The injection volume was 50 µL, and the results were evaluated at 254 nm. Changes in amino acid amounts, classified by the structural characteristics of the samples, were calculated as described by [14].

2.2.10. Lactic Acid and Short Chain Fatty Acids (SCFAs)

A Shimadzu Prominence 20ACBM high-performance liquid chromatography (HPLC) system (Japan) with an LC-20AT pump, an Inertsil ODS-4 column (250 mm × 4.6 mm, 5 µm; GP Sciences, Tokyo, Japan), and a DAD (SPD-M20A) detector was used for lactic acid analysis. The mobile phase was ultrapure water with pH adjusted to 3 using orthophosphoric acid. Before injection, samples were centrifuged and vortexed [28]. Using an Agilent 7697A headspace sampler and an Agilent 7890A GC-5975C MS system (Agilent Technologies,

Santa Clara, CA, USA), analyses of acetic, propionic, and butyric acids were carried out in accordance with the procedure suggested by [29]. This method involved maintaining the temperature at 35 °C for five minutes, then raising it to 150 °C at 50 °C per minute, where it remained for five more minutes. The flow rate was 25 psi (He), the thermostat time was 5 min, the pressure time was 0.5 min, the injection time was 0.08 min, and the draw time was 0.5 min. The detector and injector temperatures were set to 200 °C and 180 °C, respectively. Each homogeneous liquid sample was added to the headspace system in a 4-mL aliquot.

2.2.11. Statistical Analysis

The experimental design consisted of two independent fermentation batches (biological replicates) for each bacterial strain and culture medium condition. Analytical measurements were performed in triplicate within each batch, and the technical measurements were averaged to obtain one value per independent fermentation batch. These batch-level means were used as the observations for statistical analysis, with the independent fermentation batch considered the experimental unit (n = 2 per condition). Technical replicates were not treated as independent observations in the analysis of variance (ANOVA). Before statistical analysis, data screening excluded sensory attributes with a mean value of zero. Two-way analysis of variance (ANOVA) assessed the effects of medium type and fermentation period. Fisher's least significant difference (LSD) test compared means when ANOVA indicated significant differences. Differences were considered highly significant at $p < 0.01$ and significant at $p < 0.05$. Results were expressed as mean ± standard deviation.

3. Results and Discussion

3.1. Growth Kinetics

The results for the growth kinetics parameters estimated using the modified Gompertz model are presented in Table 3 and Figure 1. The modified Gompertz model described the growth data included in the fit with high accuracy. R^2 values ranged from 0.9737 to 0.9990, while RMSE values varied between approximately 0.03 and 0.15 $\log_{10}$ CFU/mL. The CLA sample stood out from the others, exhibiting the highest maximum specific growth rate (0.94 h^{-1}), the shortest lag phase (3.22 h), and the shortest doubling time (0.74 h). Conversely, the ELA sample showed the lowest maximum specific growth rate (0.47 h^{-1}), the longest lag phase (7.61 h), and the longest doubling time (1.46 h) (Table 3).

Table 3. Growth kinetics parameters and goodness-of-fit statistics estimated using the modified Gompertz model.

Samples	y_0 ($\log_{10}$ CFU/mL)	A ($\log_{10}$)	y_{max} ($\log_{10}$ CFU/mL)	r_{max} ($\log_{10}$ CFU/mL h^{-1})	μ_{max} (h^{-1})	λ (h)	g (h)	G∞	SSE	RMSE ($\log_{10}$)	R^2
CLA	6.79	2.08	8.86	0.41	0.94	3.22	0.74	6.90	0.0052	0.0274	0.9990
CLC	7.02	2.17	9.19	0.23	0.53	4.59	1.32	7.21	0.0447	0.0799	0.9903
CLR	6.87	2.03	8.90	0.31	0.72	5.12	0.96	6.74	0.0078	0.0313	0.9987
ELA	6.88	2.43	9.31	0.21	0.47	7.61	1.46	8.06	0.1985	0.1485	0.9737
ELC	7.60	2.27	9.87	0.32	0.73	4.78	0.95	7.54	0.0142	0.0421	0.9980
ELR	7.83	1.88	9.71	0.24	0.56	6.59	1.25	6.24	0.1111	0.1111	0.9805

Note: y_0: lower asymptote; A: asymptotic logarithmic increase; y_{max}: estimated upper asymptote; r_{max} (y_0 + A): maximum growth curve slope on the $\log_{10}$ scale; μ_{max}: maximum specific growth rate; λ: lag phase duration; g: doubling time; G∞: asymptotic number of generations; SSE: sum of squared errors; RMSE: root mean squared error; R^2: coefficient of determination; CLA: culture medium containing *L. acidophilus*; CLC: culture medium containing *L. casei*; CLR: culture medium containing *L. rhamnosus*; ELA: culture medium containing eggshell membrane protein and *L. acidophilus*; ELC: culture medium containing eggshell membrane protein and *L. casei*; ELR: culture medium containing eggshell membrane protein and *L. rhamnosus*.

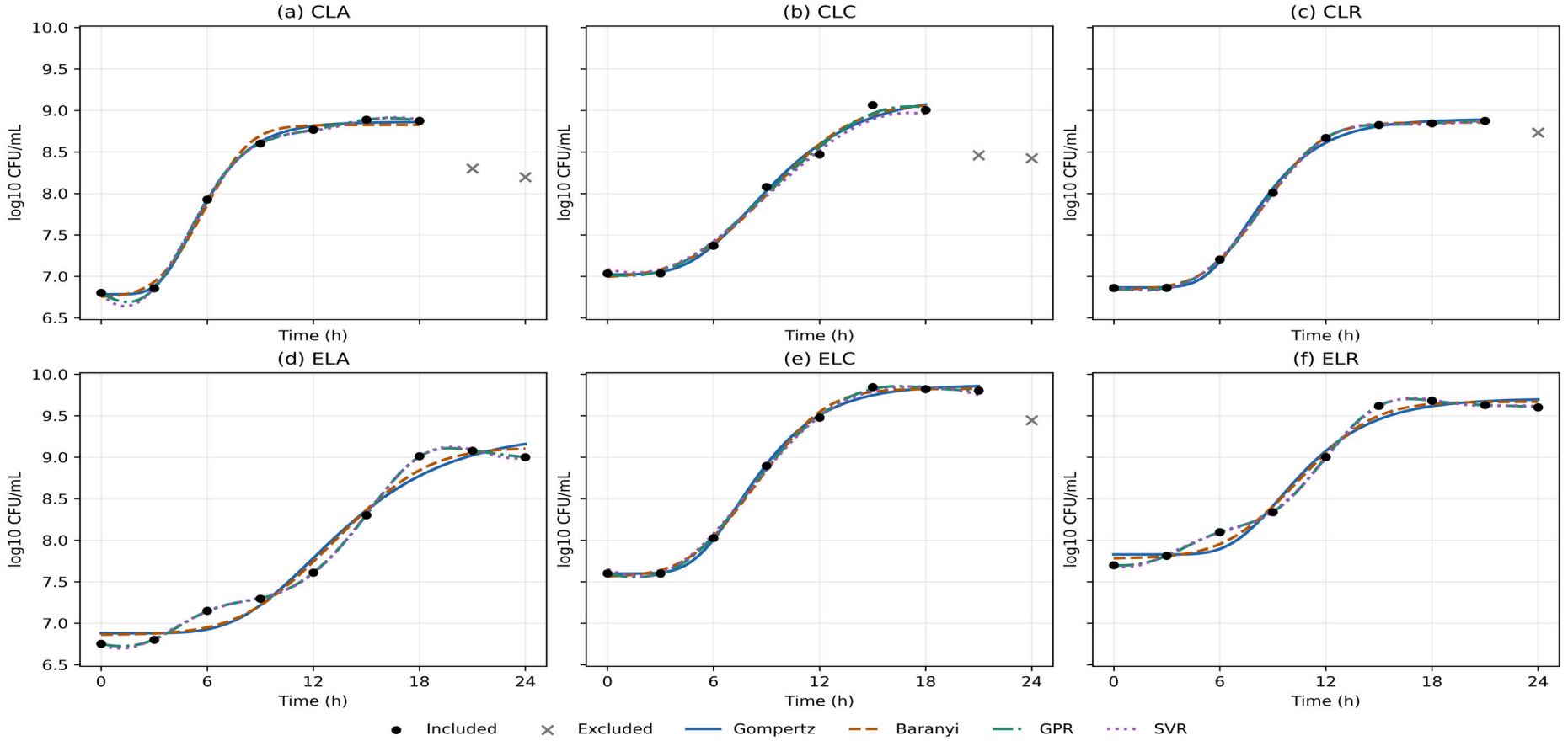


Figure 1. Observed $\log_{10}$ cell counts and fitted growth curves for (**a**) CLA, (**b**) CLC, (**c**) CLR, (**d**) ELA, (**e**) ELC, and (**f**) ELR. Black circles indicate observations included in model fitting; grey crosses indicate excluded observations. Colored lines represent the modified Gompertz, Baranyi–Roberts, GPR, and SVR models fitted to all included observations for each condition. Curves are shown only over the included time range. CLA, CLC, and CLR denote control media containing *L. acidophilus*, *L. casei*, and *L. rhamnosus*, respectively; ELA, ELC, and ELR denote the corresponding media containing eggshell membrane protein.

The highest upper asymptote was estimated for the ELC sample (9.87 $\log_{10}$ CFU/mL). ELA, on the other hand, exhibited the highest asymptotic logarithmic increase (2.43 $\log_{10}$) and the highest asymptotic number of generations (8.06). Consequently, a high maximum growth rate did not directly correspond to achieving the highest asymptotic cell count or the greatest total population increase. Since the upper asymptote includes the initial cell counts, this explains why ELC reached a higher upper asymptote, while ELA showed a greater logarithmic increase.

The higher RMSE values obtained for the ELA and ELR samples indicate that their observed growth curves deviate more significantly from the model predictions (Table 3). For *L. acidophilus*, the maximum specific growth rate decreased from 0.94 h^{-1} in CLA to 0.47 h^{-1} in ELA, while the lag phase duration extended from 3.22 h to 7.61 h. Similarly, for *L. rhamnosus*, a lower growth rate and a longer lag phase were observed in the ELR sample than in the CLR sample. In contrast, for *L. casei*, the maximum specific growth rate increased from 0.53 h^{-1} in CLC to 0.73 h^{-1} in ELC, and the lag phase durations were found to be more similar. The kinetic effect of the medium containing eggshell membrane powder did not follow the same direction for all the bacteria tested.

Bisson et al. [30] stated that the growth behaviors of probiotic *Lactobacilli*, when examined under various environmental conditions, vary by species. Consequently, for *L. acidophilus* and *L. rhamnosus*, an extended lag phase led to a longer adaptation period to changes in nutrient composition. Similarly, Ref. [31] reported that when certain probiotic *Lactobacilli* were grown in a cereal-based medium, developed as an alternative to standard culture media, their lag phases were prolonged, yet both their cell counts and growth rates increased. The finding that the estimated upper asymptote for ELC was higher than that for CLC indicates that the medium containing eggshell membrane powder supported a greater asymptotic cell density for the *L. casei* culture under investigation. The results obtained using the Baranyi–Roberts model for estimating growth kinetics are presented in Table 4 and Figure 1. It has been established that the nutritional requirements of lactic acid bacteria (LAB) vary at the species and strain levels, and that growth kinetics with alternative protein sources differ among microorganisms [32,33].

Table 4. Growth kinetic parameters and goodness-of-fit statistics estimated using the Baranyi–Roberts model.

Samples	y_0 ($\log_{10}$ CFU/mL)	y_{max} ($\log_{10}$ CFU/mL)	μ_{max} (h^{-1})	λ (h)	g (h)	G∞	SSE	RMSE ($\log_{10}$)	R^2
CLA	6.76	8.83	1.07	3.58	0.65	6.87	0.0301	0.0656	0.9942
CLC	7.00	9.08	0.60	5.22	1.16	6.93	0.0444	0.0797	0.9904
CLR	6.84	8.86	0.83	5.68	0.83	6.68	0.0014	0.0130	0.9998
ELA	6.86	9.12	0.56	8.58	1.23	7.49	0.1269	0.1188	0.9832
ELC	7.57	9.82	0.76	5.06	0.91	7.51	0.0144	0.0425	0.9979
ELR	7.78	9.67	0.64	7.08	1.09	6.27	0.0572	0.0797	0.9900

Note: y_0: lower asymptote; y_{max}: estimated upper asymptote; μ_{max}: maximum specific growth rate; λ: lag phase duration; g: doubling time; G∞: asymptotic number of generations; SSE: sum of squared errors; RMSE: root mean squared error; R^2: coefficient of determination. CLA: culture medium containing *L. acidophilus*; CLC: culture medium containing *L. casei*; CLR: culture medium containing *L. rhamnosus*; ELA: culture medium containing eggshell membrane protein and *L. acidophilus*; ELC: culture medium containing eggshell membrane protein and *L. casei*; ELR: culture medium containing eggshell membrane protein and *L. rhamnosus*.

For *L. acidophilus*, the maximum specific growth rate (μ_{max}) was 1.07 h^{-1} in the standard MRS medium, whereas this value decreased to 0.56 h^{-1} in the medium containing eggshell membrane (ESM). The lag phase increased from 3.58 to 8.58 h, and the generation time increased from 0.66 to 1.24 h. Consequently, in the medium containing eggshell membrane,

both the adaptation of *L. acidophilus* to the new environment and its exponential proliferation were slower than in the control medium. Baranyi and Roberts [24] state that the lag phase is the combined result of the inoculum's initial physiological state and the environmental conditions encountered after inoculation. Therefore, the prolonged lag phase observed in an eggshell membrane medium may be linked to an additional metabolic adaptation requirement stemming from a reduction in readily available peptide and amino acid sources. The maximum population size and the number of generations for *L. acidophilus* were higher in the eggshell membrane medium. Although eggshell membrane powder reduces the growth rate of *L. acidophilus*, it can support a high cell density over a long incubation period. These findings may be attributed to the eggshell membrane being a complex biological material composed of collagen-like and other fibrous proteins, as well as keratin, glycoproteins, and glycosaminoglycans [34].

It has been determined that the μ_{max} value for *L. casei* is higher in the presence of eggshell membrane. These results indicate that the adaptation of *L. casei* to an environment containing eggshell membrane is not negatively affected; on the contrary, its exponential growth capacity is enhanced compared to that in the control medium. Furthermore, *L. casei* was identified as the bacterium that adapts most effectively to the presence of eggshell membrane. Studies comparing the proteolytic systems of lactic acid bacteria at the genomic level reveal significant variations among species regarding the composition of their proteinase, peptidase, and peptide transport systems [35]. Such differences may explain why, in the present study, *L. casei* was able to metabolize eggshell membrane more efficiently than *L. acidophilus* or *L. rhamnosus* (Table 4). The strain-dependent responses to ESM-containing media may be associated with differences in nutrient availability, proteolytic activity, and metabolic adaptation. Lactic acid bacteria possess proteolytic systems that facilitate the utilization of proteins and peptides through extracellular proteinases, peptide transport systems, and intracellular peptidases. However, the complex and cross-linked protein structure of ESM may limit the immediate availability of nitrogenous compounds compared with conventional nutrient sources. Differences in the capacity of bacterial strains to utilize these substrates may therefore contribute to the observed variations in maximum specific growth rate and lag phase duration. The increased growth rate observed for *L. casei* suggests a more favorable response to the modified nutrient composition, whereas the prolonged adaptation periods of *L. acidophilus* and *L. rhamnosus* may reflect differences in their nutritional requirements and metabolic adaptation.

For *L. rhamnosus*, the use of eggshell membrane resulted in growth kinetics that differed from those observed for *L. casei*. The maximum specific growth rate decreased from 0.83 h^{-1} to 0.64 h^{-1}, while the lag phase lengthened and the generation time increased. These results indicate that the adaptation and cell division rate of *L. rhamnosus* in an eggshell membrane-containing medium are lower than in the control medium. Conversely, the maximum cell counts of *L. rhamnosus* increased in the presence of the eggshell membrane (Table 4).

In their study, they reported that eggshell membrane proteins can be hydrolyzed to produce protein hydrolysates through fermentation with *L. plantarum*. This supports the findings of the present study by demonstrating that lactic acid bacteria (LAB) can exhibit proteolytic activity on the protein matrix of the eggshell membrane, and that the eggshell membrane can serve as a biological substrate for microbial fermentation [12].

From a biological perspective, both the modified Gompertz and Baranyi–Roberts models provided consistent insights into the strain-dependent effects of ESM-containing media on bacterial growth (Tables 3 and 4). The maximum specific growth rate (μ_{max}) reflects bacterial proliferation during the exponential phase, while the lag phase (λ) represents the adaptation period, and the estimated maximum cell count (y_{max}) indicates the population level supported under the modeled conditions. Both models showed that ESM-containing

media increased μ_{max} for *L. casei* but decreased it for *L. acidophilus* and *L. rhamnosus*. Similarly, prolonged lag phases were observed for *L. acidophilus* and *L. rhamnosus*, whereas the lag phase of *L. casei* showed only minor model-dependent differences. Interestingly, despite their reduced growth rates, *L. acidophilus* and *L. rhamnosus* exhibited higher estimated maximum cell densities in ESM-containing media. These findings indicate that slower adaptation and exponential growth do not necessarily result in lower asymptotic population levels. The overall agreement between the two kinetic models strengthens the descriptive interpretation of strain-specific growth responses, highlighting the importance of considering growth rate, adaptation time, and maximum cell density together rather than relying solely on goodness-of-fit statistics. In the growth approach developed by Baranyi and Roberts [24], parameters such as initial population, maximum population, maximum specific growth rate, and lag phase can be used to define the fundamental kinetic characteristics of microbial growth. The Baranyi–Roberts model described the included growth observations with R^2 values of 0.9832–0.9998 and RMSE values of 0.0130–0.1188 $\log_{10}$ CFU/mL. The lowest fitting error was observed for CLR ($R^2 = 0.9998$; RMSE = 0.0130), whereas ELA showed the highest error ($R^2 = 0.9832$; RMSE = 0.1188). These statistics describe agreement with the observations used for fitting and do not establish predictive performance at unobserved time points. The contrasting responses of the three probiotic strains indicate that the suitability of ESM-containing media depends strongly on the microorganism and the intended fermentation outcome. Among the investigated strains, *L. casei* showed the most favorable kinetic response, with increased maximum specific growth rate and estimated maximum cell density, suggesting its potential suitability for fermentation processes aimed at achieving high viable cell populations. In contrast, *L. acidophilus* and *L. rhamnosus* exhibited reduced growth rates and prolonged lag phases despite reaching higher estimated asymptotic cell counts. These responses suggest that ESM-containing media may be less suitable when rapid bacterial proliferation and short fermentation times are required. Nevertheless, the substantial amino acid accumulation observed in the ESM-containing *L. acidophilus* culture indicates that growth performance and metabolite characteristics should be considered separately when evaluating potential applications. Importantly, because ESM replaced conventional complex nitrogen sources, the observed differences reflect changes in the overall nutrient composition rather than the isolated effect of ESM. Therefore, strain-specific optimization and further validation are necessary before recommending ESM-containing media for practical fermentation applications.

3.2. Comparison with Machine Learning Models

GPR and SVR were compared with the two primary growth models using the same included observations and validation procedure (Figure 1; Table 5). Across the six culture conditions, GPR yielded the lowest mean CV_RMSE (0.1344 $\log_{10}$ CFU/mL), followed closely by SVR (0.1359), Baranyi–Roberts (0.1533), and modified Gompertz (0.1657). Linear interpolation gave a mean CV_RMSE of 0.1839. The mean CV_MAE and CV_R^2 values also favored GPR. However, the lowest condition-specific CV_RMSE was obtained with modified Gompertz for CLA, CLC and ELC, Baranyi–Roberts for CLR, SVR for ELA, and GPR for ELR.

Close agreement with the fitting observations did not consistently translate into lower validation error. For CLA, for example, GPR had a fitting RMSE below 0.0001 $\log_{10}$ CFU/mL, but its CV_RMSE was 0.2075, compared with 0.0875 for modified Gompertz (Figure 2). The results therefore support a condition-dependent choice of model rather than uniform superiority of the machine learning methods. Their contribution was most evident for ELA and ELR, where both GPR and SVR reduced interpolation error relative to the primary models.

Table 5. Prediction performance at withheld intermediate time points.

Condition/Metric	Modified Gompertz	Baranyi–Roberts	GPR	SVR	Linear Interpolation
CLA	0.0875	0.2508	0.2075	0.2453	0.2713
CLC	0.1551	0.1901	0.2083	0.2077	0.2032
CLR	0.1274	0.0184	0.0396	0.0433	0.1614
ELA	0.2754	0.2158	0.1226	0.0925	0.1628
ELC	0.0778	0.0923	0.1102	0.0999	0.1666
ELR	0.2707	0.1522	0.1180	0.1265	0.1382
Mean CV_RMSE	0.1657	0.1533	0.1344	0.1359	0.1839
Mean CV_MAE	0.1404	0.1333	0.1120	0.1256	0.1520
Mean CV_R^2	0.9444	0.9504	0.9630	0.9593	0.9404

Note: Condition-specific entries are CV_RMSE values. CV_RMSE and CV_MAE are in $\log_{10}$ CFU/mL; CV_R^2 is dimensionless. Mean scores are unweighted averages across the six conditions. Five intermediate points were withheld for CLA and CLC, six for CLR and ELC, and seven for ELA and ELR. Lower errors and higher CV_R^2 indicate better performance. No significance tests were applied to model differences.

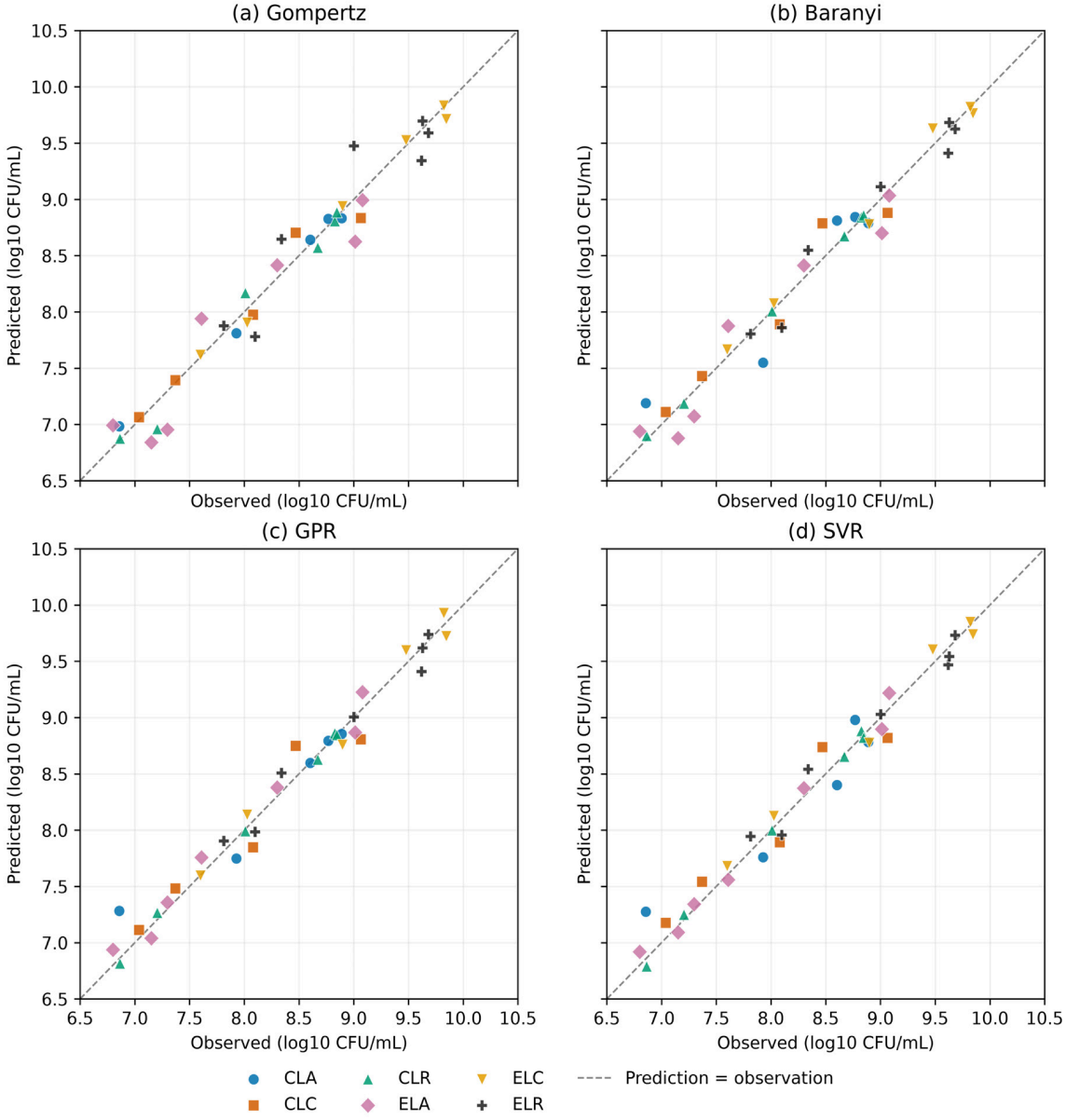


Figure 2. Observed and predicted $\log_{10}$ cell counts at withheld intermediate time points for (**a**) modified Gompertz, (**b**) Baranyi–Roberts, (**c**) GPR, and (**d**) SVR. Each panel contains 36 predictions

obtained by refitting the model without the corresponding observation. Colors and symbols identify the six culture conditions defined in Figure 1. The dashed line indicates equality between observed and predicted values; all panels use identical axis limits and equal axis scaling.

Modified Gompertz and Baranyi–Roberts models provide interpretable estimates of lag time, maximum specific growth rate, and asymptotic cell counts, but these estimates depend on the assumed curve structure and adequate coverage of the growth phases. GPR and SVR offer flexible interpolation without prescribing a sigmoidal equation, but do not directly estimate these kinetic parameters in the present implementation. With only seven to nine included observations per curve, both approaches may be sensitive to individual observations and modelling choices. The small difference in mean CV_RMSE between GPR and SVR does not establish a practically meaningful or statistically significant advantage.

It should be emphasized that the predictive performance reported in this study refers specifically to interpolation within the experimentally observed growth curves. Although the models were able to describe the measured growth patterns and estimate withheld intermediate observations, their performance cannot be generalized to different fermentation conditions without additional experimental validation. Therefore, the present findings demonstrate the comparative interpolation capabilities of the evaluated models rather than their ability to predict microbial growth under previously untested environmental or nutritional conditions.

3.3. pH

In all samples, the pH generally decreased throughout the incubation period, reaching a range of 3.58–5.20 at the 24th hour. At the end of fermentation, the lowest pH was observed in the CLR sample (3.58), while the highest was observed in the ELA sample (5.20). Although there were no significant differences between CLA–CLC and ELA–ELC at the beginning, all samples differed from one another at every measurement point from the 3rd hour onwards (Table 6, Fisher LSD, $p < 0.05$).

Samples containing eggshell membrane powder exhibited higher pH values at all measurement times compared to their respective controls (samples of the same species in a control medium). The difference in pH between the start and end of fermentation was greater in the control medium for *L. acidophilus* and *L. casei*, whereas for *L. rhamnosus*, the difference was similar in both media. This indicates that responses to changes in the growth environment can vary by species. The decline in pH reflects increased acidity during fermentation; however, it is influenced not only by the organic acids produced but also by the medium's buffering capacity. The decrease in pH during fermentation can be primarily attributed to the metabolic activity of lactic acid bacteria, which utilize glucose and other available fermentable carbohydrates and convert them into organic acids, predominantly lactic acid. The accumulation of these acidic metabolites increases the hydrogen ion concentration in the fermentation medium, resulting in a gradual reduction in pH. However, the extent of acidification depends on the metabolic characteristics of the bacterial strain, substrate utilization, and the buffering capacity of the medium. The consistently higher pH values observed in ESM-containing media compared with their respective controls may therefore be associated with differences in organic acid metabolism and the buffering properties of the medium components.

Table 6. Results for pH values throughout fermentation.

Time (h)	0	3	6	9	12	15	18	21	24
CLA	6.75 ± 0.014 ^{c}	5.99 ± 0.007 ^{c}	5.92 ± 0.007 ^{c}	4.45 ± 0.014 ^{e}	4.36 ± 0.007 ^{d}	4.25 ± 0.042 ^{d}	4.18 ± 0.014 ^{d}	4.08 ± 0.000 ^{d}	4.10 ± 0.007 ^{d}
CLC	6.75 ± 0.007 ^{c}	5.93 ± 0.000 ^{d}	5.21 ± 0.000 ^{e}	4.57 ± 0.014 ^{d}	4.19 ± 0.014 ^{e}	4.06 ± 0.021 ^{e}	3.91 ± 0.021 ^{e}	3.80 ± 0.000 ^{e}	3.78 ± 0.007 ^{e}
CLR	6.69 ± 0.014 ^{d}	4.66 ± 0.007 ^{f}	4.00 ± 0.007 ^{f}	3.79 ± 0.007 ^{f}	3.70 ± 0.007 ^{f}	3.67 ± 0.007 ^{f}	3.62 ± 0.007 ^{f}	3.59 ± 0.014 ^{f}	3.58 ± 0.000 ^{f}
ELA	7.38 ± 0.000 ^{a}	6.59 ± 0.000 ^{b}	6.24 ± 0.014 ^{a}	6.19 ± 0.000 ^{a}	6.26 ± 0.007 ^{a}	6.11 ± 0.007 ^{a}	5.79 ± 0.014 ^{a}	5.50 ± 0.000 ^{a}	5.20 ± 0.000 ^{a}
ELC	7.39 ± 0.000 ^{a}	6.70 ± 0.007 ^{a}	6.08 ± 0.007 ^{b}	5.62 ± 0.000 ^{b}	5.45 ± 0.000 ^{b}	5.26 ± 0.007 ^{b}	5.13 ± 0.007 ^{b}	5.00 ± 0.007 ^{b}	4.91 ± 0.007 ^{b}
ELR	7.26 ± 0.028 ^{b}	5.72 ± 0.000 ^{e}	5.24 ± 0.000 ^{d}	4.94 ± 0.007 ^{c}	4.87 ± 0.000 ^{c}	4.71 ± 0.007 ^{c}	4.76 ± 0.052 ^{c}	4.63 ± 0.000 ^{c}	4.56 ± 0.000 ^{c}

Note: Values are expressed as mean ± standard deviation (SD). Different lowercase superscript letters within the same column indicate statistically significant differences among culture media at the same fermentation time ($p < 0.05$, Fisher's LSD test). CLA: culture medium containing *L. acidophilus*; CLC: culture medium containing *L. casei*; CLR: culture medium containing *L. rhamnosus*; ELA: culture medium containing eggshell membrane protein and *L. acidophilus*; ELC: culture medium containing eggshell membrane protein and *L. casei*; ELR: culture medium containing eggshell membrane protein and *L. rhamnosus*.

3.4. Changes in the Amino Acid Composition

ESM, a protein-rich (~90%) by-product of egg processing technology, contains functional proteins such as lysozyme, collagen, and ovotransferrin, as well as bioactive peptides [36]. Rich in cysteine, the amino acid composition of ESM also features high levels of aromatic (tyrosine, phenylalanine), sulfur-containing (cysteine, methionine), and basic (histidine, lysine, arginine) amino acids [37].

Tables 7 and 8 present, respectively, the free amino acid contents and the proportions of amino acids classified by structural characteristics for the culture medium samples. An evaluation of the free amino acid profiles of the CLA, CLC, CLR, ELA, ELC, and ELR samples reveals that both the fermentation duration and the culture medium composition exert distinct effects on these profiles (Table 7). It is believed that both the metabolic characteristics of the microorganisms and the addition of eggshell membrane influence the observed changes in the amino acid profile. Through the action of protease and peptidase enzymes produced by lactic acid bacteria (LAB), proteins are hydrolyzed into peptides and amino acids; this proteolytic activity varies with the specific species and strain [22,38].

At the end of fermentation, the ELA sample exhibited the highest concentrations of Ile, Phe, Asp, Glu, His, Lys, and Cys among the investigated samples (Table 7). However, Arg concentration decreased from 72.14 to 64.78 mg/kg during fermentation, indicating that arginine consumption also occurred in this medium (Table 7, $p < 0.01$). In their study investigating the effect of probiotic bacteria on the proteolysis of semi-hard cheese, Bergamini et al. [39] noted that different strains of *L. acidophilus* and *L. casei* contribute differently to proteolysis and the formation of free amino acids; specifically, *L. acidophilus* strains exhibited more pronounced peptidolytic activity and a greater increase in free amino acids. Glu, Asp, Cys, and Pro are among the primary amino acid components of eggshell membrane [40].

A study by [12] reported that hydrolysates obtained by fermenting ESM with *Lactobacillus plantarum* contain 21.4% hydrophobic amino acids (Ile, Leu, Trp, Pro, Met, Cys, Val, Tyr, Ala, and Phe) and 3.6% aromatic amino acids (Phe, Tyr, and Trp). It was further noted that these fermented hydrolysates contain a significant proportion of essential amino acids (15.41%; Leu, Ile, His, Met, Lys, Phe, Val, Trp, and Thr) and have potential for use in various food applications.

The Arg level decreased significantly in all samples—CLA, CLC, CLR, ELA, ELC, and ELR—after 24 h of fermentation (Table 7, $p < 0.01$). Arginine can be catabolized by lactic acid bacteria (LAB) via the arginine deiminase (ADI) pathway, converting it into citrulline and subsequently into ornithine; this process generates ammonia and ATP. Thus, arginine metabolism contributes to meeting the energy requirements of the cells and facilitating their adaptation to acid stress, particularly under acidic conditions. The genetic components of the ADI pathway are present within the genome of LAB [41]. Various studies have also noted that arginine levels decline during fermentation, as it is utilized by many LAB as an energy source [42–44].

LAB require various free amino acids for their intracellular metabolism. Furthermore, the proteinases involved in hydrolysis may exhibit substrate-specific differences [14,45]. It is hypothesized that different bacteria possess varying capacities to utilize the matrix in culture media supplemented with eggshell membrane, a substance rich in collagen, keratin, and other structural proteins.

Table 7. Changes in the amino acid contents of the samples (mg/kg).

Samples	CLA		CLC		CLR		ELA		ELC		ELR	
FT	**0**	**24**	**0**	**24**	**0**	**24**	**0**	**24**	**0**	**24**	**0**	**24**
Arg	132.18 ± 3.930 ^{bA}	64.85 ± 1.780 ^{aB}	133.95 ± 3.410 ^{bA}	53.89 ± 2.000 ^{bB}	142.57 ± 5.210 ^{aA}	27.80 ± 0.841 ^{dB}	72.14 ± 3.350 ^{dA}	64.78 ± 2.820 ^{aB}	59.80 ± 1.508 ^{eA}	39.20 ± 1.810 ^{cB}	83.54 ± 2.220 ^{cA}	39.44 ± 1.162 ^{cB}
Ser	6.53 ± 0.223 ^{dA}	3.09 ± 0.076 ^{cB}	2.46 ± 0.075 ^{eA}	1.69 ± 0.084 ^{dB}	1.53 ± 0.043 ^{eB}	2.70 ± 0.096 ^{cA}	26.66 ± 1.205 ^{aA}	9.12 ± 0.447 ^{bB}	9.99 ± 0.457 ^{bA}	0.95 ± 0.041 ^{eB}	7.93 ± 0.222 ^{cB}	9.57 ± 0.283 ^{aA}
Gly	14.48 ± 0.450 ^{bA}	10.62 ± 0.366 ^{bB}	6.42 ± 0.182 ^{dB}	25.43 ± 0.683 ^{aA}	8.50 ± 0.315 ^{cA}	2.98 ± 0.117 ^{eB}	4.06 ± 0.119 ^{eB}	9.57 ± 0.327 ^{cA}	8.93 ± 0.243 ^{cA}	3.26 ± 0.139 ^{eB}	18.10 ± 0.415 ^{aA}	6.43 ± 0.261 ^{dB}
Ala	14.03 ± 0.628 ^{aA}	2.91 ± 0.079 ^{eB}	0.87 ± 0.040 ^{dB}	3.56 ± 0.138 ^{dA}	3.16 ± 0.074 ^{bB}	16.65 ± 0.626 ^{aA}	1.00 ± 0.050 ^{dB}	2.35 ± 0.105 ^{eA}	0.75 ± 0.017 ^{dB}	13.52 ± 0.573 ^{bA}	1.96 ± 0.066 ^{cB}	5.32 ± 0.125 ^{cA}
Pro	1.26 ± 0.058 ^{dB}	2.50 ± 0.052 ^{bA}	0.79 ± 0.036 ^{eB}	0.91 ± 0.032 ^{eA}	1.21 ± 0.051 ^{dB}	1.70 ± 0.038 ^{dA}	1.51 ± 0.035 ^{cB}	1.91 ± 0.075 ^{cA}	2.32 ± 0.054 ^{aA}	1.90 ± 0.075 ^{cB}	1.70 ± 0.064 ^{bB}	3.67 ± 0.172 ^{aA}
GABA	0.52 ± 0.014 ^{cB}	3.42 ± 0.159 ^{aA}	1.12 ± 0.055 ^{bA}	0.48 ± 0.015 ^{dB}	1.21 ± 0.056 ^{bA}	0.82 ± 0.023 ^{cB}	0.67 ± 0.015 ^{cA}	0.43 ± 0.010 ^{dB}	4.28 ± 0.213 ^{aA}	2.51 ± 0.078 ^{bB}	1.18 ± 0.046 ^{bA}	0.80 ± 0.028 ^{cB}
Val	43.39 ± 1.186 ^{dB}	98.41 ± 2.650 ^{aA}	1.82 ± 0.051 ^{eB}	35.51 ± 1.064 ^{bA}	70.21 ± 2.480 ^{aA}	1.51 ± 0.071 ^{dB}	66.69 ± 1.543 ^{bA}	7.98 ± 0.265 ^{cB}	52.41 ± 2.330 ^{cA}	3.02 ± 0.099 ^{dB}	69.28 ± 2.650 ^{abA}	1.11 ± 0.042 ^{dB}
Thr	1.84 ± 0.086 ^{dB}	25.26 ± 0.538 ^{bA}	2.03 ± 0.073 ^{cA}	1.83 ± 0.048 ^{cA}	2.62 ± 0.104 ^{aA}	2.38 ± 0.049 ^{cA}	2.31 ± 0.081 ^{bA}	2.13 ± 0.060 ^{cA}	2.76 ± 0.089 ^{aB}	116.22 ± 3.840 ^{aA}	2.42 ± 0.100 ^{bA}	2.76 ± 0.069 ^{cA}
Met	10.06 ± 0.223 ^{dA}	8.86 ± 0.202 ^{bcA}	12.42 ± 0.553 ^{bA}	12.56 ± 0.556 ^{aA}	14.89 ± 0.525 ^{aA}	8.01 ± 0.386 ^{dB}	7.71 ± 0.177 ^{eB}	8.40 ± 0.257 ^{cdB}	9.08 ± 0.443 ^{eA}	9.34 ± 0.418 ^{bA}	11.10 ± 0.442 ^{cA}	9.23 ± 0.390 ^{bB}
Ile	0.87 ± 0.022 ^{eA}	0.60 ± 0.019 ^{eA}	0.80 ± 0.022 ^{eA}	0.85 ± 0.030 ^{eA}	1.59 ± 0.050 ^{dB}	2.47 ± 0.094 ^{dA}	6.83 ± 0.150 ^{bB}	18.07 ± 0.596 ^{aA}	5.59 ± 0.233 ^{cA}	4.73 ± 0.224 ^{cB}	7.38 ± 0.163 ^{aA}	6.84 ± 0.282 ^{bB}
Leu	9.27 ± 0.391 ^{bA}	6.78 ± 0.245 ^{cB}	8.27 ± 0.354 ^{cB}	11.00 ± 0.374 ^{aA}	9.79 ± 0.237 ^{bA}	3.22 ± 0.147 ^{eB}	8.11 ± 0.398 ^{cB}	10.33 ± 0.310 ^{bA}	6.69 ± 0.154 ^{dA}	3.27 ± 0.098 ^{eB}	18.39 ± 0.704 ^{aA}	4.83 ± 0.127 ^{dB}
Phe	13.92 ± 0.512 ^{cA}	2.89 ± 0.066 ^{eB}	15.85 ± 0.425 ^{bA}	3.25 ± 0.108 ^{dB}	19.92 ± 0.547 ^{aA}	6.53 ± 0.249 ^{bB}	12.84 ± 0.261 ^{dA}	11.70 ± 0.321 ^{aB}	1.95 ± 0.096 ^{eB}	3.71 ± 0.109 ^{cA}	1.95 ± 0.085 ^{eA}	2.18 ± 0.047 ^{fA}
Tyr	2.02 ± 0.047 ^{cB}	255.31 ± 10.490 ^{dA}	2.85 ± 0.063 ^{cA}	29.08 ± 1.083 ^{eA}	1.65 ± 0.071 ^{cA}	5.39 ± 0.149 ^{eA}	0.96 ± 0.031 ^{cB}	508.34 ± 13.680 ^{cA}	445.88 ± 20.900 ^{bB}	778.14 ± 34.400 ^{bA}	758.70 ± 25.300 ^{aB}	1183.67 ± 40.300 ^{aA}
Trp	4.71 ± 0.097 ^{cB}	5.96 ± 0.187 ^{bA}	6.67 ± 0.281 ^{bA}	1.61 ± 0.074 ^{eB}	3.03 ± 0.099 ^{dB}	5.23 ± 0.124 ^{cA}	10.88 ± 0.282 ^{aA}	5.45 ± 0.250 ^{cB}	2.52 ± 0.083 ^{eB}	3.64 ± 0.151 ^{dA}	3.12 ± 0.063 ^{dB}	11.57 ± 0.511 ^{aA}
Asp	0.07 ± 0.003 ^{bA}	0.52 ± 0.020 ^{bA}	0.71 ± 0.020 ^{bA}	0.07 ± 0.002 ^{eA}	0.69 ± 0.018 ^{bA}	0.18 ± 0.005 ^{dA}	0.25 ± 0.009 ^{bA}	0.77 ± 0.025 ^{aA}	265.21 ± 11.070 ^{aA}	0.46 ± 0.021 ^{cB}	0.08 ± 0.003 ^{bA}	0.09 ± 0.003 ^{eA}
Glu	1.49 ± 0.057 ^{fB}	2.24 ± 0.059 ^{cA}	13.67 ± 0.366 ^{aA}	1.52 ± 0.037 ^{dB}	5.04 ± 0.228 ^{cA}	2.13 ± 0.095 ^{cB}	8.54 ± 0.196 ^{bA}	22.22 ± 0.557 ^{aA}	2.21 ± 0.079 ^{eB}	9.73 ± 0.310 ^{bA}	2.93 ± 0.135 ^{dA}	2.47 ± 0.055 ^{cB}
His	90.74 ± 1.940 ^{dA}	119.86 ± 4.320 ^{cA}	77.52 ± 3.390 ^{eA}	76.87 ± 2.920 ^{cA}	122.81 ± 5.800 ^{abA}	97.65 ± 2.450 ^{cA}	112.60 ± 3.230 ^{cB}	2086.62 ± 69.100 ^{aA}	128.94 ± 6.390 ^{aB}	584.70 ± 25.300 ^{bA}	116.18 ± 4.960 ^{bcA}	119.54 ± 3.250 ^{cA}
Lys	0.48 ± 0.018 ^{abA}	0.47 ± 0.022 ^{cdA}	0.45 ± 0.012 ^{bcA}	0.46 ± 0.010 ^{cdA}	0.46 ± 0.022 ^{bcA}	0.42 ± 0.011 ^{dA}	0.51 ± 0.020 ^{aB}	2.38 ± 0.103 ^{aA}	0.46 ± 0.022 ^{bcB}	1.64 ± 0.051 ^{bA}	0.44 ± 0.022 ^{cA}	0.52 ± 0.022 ^{cA}
Cys	0.63 ± 0.017 ^{cB}	0.88 ± 0.020 ^{bA}	1.09 ± 0.030 ^{bA}	0.61 ± 0.020 ^{dB}	1.08 ± 0.025 ^{bA}	0.55 ± 0.020 ^{eB}	0.64 ± 0.020 ^{cB}	1.12 ± 0.030 ^{aA}	3.08 ± 0.060 ^{aA}	0.81 ± 0.020 ^{cB}	0.46 ± 0.020 ^{dA}	0.49 ± 0.020 ^{fA}

Note: Different lowercase superscript letters represent significant differences ($p < 0.01$) among media, whereas different uppercase superscript letters represent significant differences ($p < 0.01$) between the fermentation times. CLA: culture medium containing *L. acidophilus*; CLC: culture medium containing *L. casei*; CLR:

culture medium containing *L. rhamnosus*; ELA: culture medium containing eggshell membrane protein and *L. acidophilus*; ELC: culture medium containing eggshell membrane protein and *L. casei*; ELR: culture medium containing eggshell membrane protein and *L. rhamnosus*; FT: fermentation time.

Table 8. Changes in amino acid amounts classified according to structural characteristics of the samples (mg/kg).

Samples	FT	TAA	EAA	NEAA	BAA	HBAA	HLAA	AAA	SAA	ACAA	PAA	NPAA
CLA	0	348.51 ± 9.890 ^{dB}	175.27 ± 4.480 ^{dB}	173.23 ± 5.410 ^{cB}	223.41 ± 5.890 ^{bA}	99.06 ± 3.330 ^{bB}	140.76 ± 4.230 ^{bA}	20.65 ± 0.656 ^{cB}	10.69 ± 0.224 ^{dA}	1.57 ± 0.050 ^{cB}	21.08 ± 0.579 ^{cB}	111.99 ± 3.570 ^{cB}
	24	615.40 ± 21.300 ^{dA}	269.08 ± 8.250 ^{cA}	346.34 ± 13.090 ^{dA}	187.17 ± 6.120 ^{cB}	149.97 ± 4.020 ^{aA}	71.17 ± 1.950 ^{bB}	264.16 ± 10.740 ^{dA}	9.74 ± 0.213 ^{bB}	2.76 ± 0.079 ^{cA}	293.39 ± 11.310 ^{dA}	139.53 ± 3.870 ^{aA}
CLC	0	289.75 ± 9.430 ^{eA}	125.83 ± 5.170 ^{eB}	163.92 ± 4.270 ^{cA}	211.91 ± 6.820 ^{bcA}	36.84 ± 1.183 ^{dB}	151.23 ± 3.890 ^{bA}	25.38 ± 0.769 ^{cB}	13.51 ± 0.569 ^{bA}	14.38 ± 0.386 ^{bA}	20.85 ± 0.779 ^{cB}	53.91 ± 1.940 ^{eB}
	24	261.17 ± 9.270 ^{eB}	143.93 ± 5.180 ^{dA}	117.24 ± 4.090 ^{eB}	131.22 ± 4.930 ^{cdB}	82.34 ± 2.480 ^{bA}	57.63 ± 2.130 ^{cB}	33.94 ± 1.265 ^{eA}	13.17 ± 0.566 ^{aA}	1.58 ± 0.039 ^{dB}	45.77 ± 1.780 ^{eA}	94.68 ± 3.060 ^{bA}
CLR	0	411.94 ± 15.940 ^{cA}	245.32 ± 9.860 ^{aA}	166.63 ± 6.080 ^{cA}	265.83 ± 11.030 ^{aA}	117.00 ± 3.860 ^{aA}	150.28 ± 5.520 ^{bA}	24.60 ± 0.574 ^{cA}	15.97 ± 0.535 ^{aA}	5.73 ± 0.246 ^{cA}	21.77 ± 0.753 ^{cA}	132.90 ± 4.380 ^{aA}
	24	188.30 ± 5.580 ^{eB}	127.41 ± 3.580 ^{dB}	60.90 ± 2.000 ^{fB}	125.88 ± 3.300 ^{dB}	37.43 ± 1.391 ^{dB}	33.22 ± 1.048 ^{eB}	17.14 ± 0.522 ^{eB}	8.56 ± 0.396 ^{cB}	2.30 ± 0.100 ^{cB}	19.02 ± 0.690 ^{eB}	48.29 ± 1.850 ^{deB}
ELA	0	344.90 ± 11.170 ^{dB}	228.47 ± 6.140 ^{bB}	116.42 ± 5.020 ^{dB}	185.25 ± 6.600 ^{eB}	103.34 ± 2.640 ^{bA}	108.10 ± 4.780 ^{cA}	24.67 ± 0.574 ^{cB}	8.35 ± 0.188 ^{eB}	8.79 ± 0.205 ^{bcB}	38.28 ± 1.504 ^{cB}	119.61 ± 3.010 ^{cA}
	24	2773.70 ± 89.300 ^{aA}	2153.10 ± 71.200 ^{aA}	620.60 ± 18.100 ^{cA}	2153.80 ± 72.000 ^{aA}	64.04 ± 2.060 ^{cB}	99.27 ± 3.950 ^{aA}	525.49 ± 14.250 ^{cA}	9.52 ± 0.273 ^{bA}	22.98 ± 0.582 ^{aA}	529.11 ± 14.460 ^{cA}	75.75 ± 2.510 ^{cB}
ELC	0	1012.90 ± 44.400 ^{bB}	210.42 ± 9.840 ^{cB}	802.50 ± 34.600 ^{aA}	189.21 ± 7.920 ^{deB}	81.41 ± 3.220 ^{cB}	337.67 ± 13.140 ^{aA}	450.30 ± 21.200 ^{bB}	12.16 ± 0.476 ^{cA}	267.42 ± 11.150 ^{aA}	470.80 ± 21.900 ^{bB}	90.25 ± 3.650 ^{dA}
	24	1580.80 ± 67.700 ^{bA}	730.30 ± 30.300 ^{bA}	850.50 ± 37.400 ^{bA}	625.50 ± 27.200 ^{bA}	149.63 ± 5.160 ^{aA}	51.98 ± 2.230 ^{dB}	785.50 ± 34.600 ^{bA}	10.15 ± 0.428 ^{bB}	10.19 ± 0.331 ^{bB}	905.50 ± 38.700 ^{bA}	46.39 ± 1.890 ^{eB}
ELR	0	1106.80 ± 37.600 ^{aB}	230.21 ± 9.190 ^{bA}	876.60 ± 28.500 ^{aB}	200.16 ± 7.200 ^{cdA}	121.13 ± 4.240 ^{aA}	94.92 ± 2.600 ^{dA}	763.80 ± 25.400 ^{aB}	11.55 ± 0.452 ^{cA}	3.01 ± 0.138 ^{cA}	780.60 ± 26.100 ^{aB}	132.92 ± 4.650 ^{aA}
	24	1410.50 ± 47.100 ^{cA}	158.57 ± 4.740 ^{dB}	1251.90 ± 42.400 ^{aA}	159.50 ± 4.430 ^{cdB}	33.14 ± 1.125 ^{dB}	52.08 ± 1.525 ^{dB}	1197.40 ± 40.800 ^{aA}	9.72 ± 0.400 ^{bB}	2.55 ± 0.058 ^{cB}	1205.70 ± 41.000 ^{aA}	51.17 ± 1.960 ^{dB}

Note: Different lowercase superscript letters represent significant differences ($p < 0.01$) among media, whereas different uppercase superscript letters represent significant differences ($p < 0.01$) between the fermentation times. CLA: culture medium containing *L. acidophilus*; CLC: culture medium containing *L. casei*; CLR: culture medium containing *L. rhamnosus*; ELA: culture medium containing eggshell membrane protein and *L. acidophilus*; ELC: culture medium containing eggshell membrane protein and *L. casei*; ELR: culture medium containing eggshell membrane protein and *L. rhamnosus*; TAA: total amino acid; EAA: essential amino acid; NEAA: non-essential amino acid; BAA: basic amino acid; HBAA: hydrophobic amino acid; HLAA: hydrophilic amino acid; AAA: aromatic amino acid; SAA: sulfurous amino acid; ACAA: acidic amino acid; PAA: polar amino acid; NPAA: nonpolar amino acid; FT: fermentation time.

At the end of fermentation, the CLA sample was characterized by increases in GABA and Val, whereas Arg decreased from 132.18 to 64.85 mg/kg. In the CLC sample, Gly and Leu concentrations increased, while Met showed no change. The ELA sample exhibited marked increases in His and Ile. In the ELC sample, Thr and His concentrations increased, whereas Pro, GABA, Asp, and Cys decreased during fermentation. The ELR sample was characterized by increases in Ser, Pro, Tyr, and Trp. In the CLR sample, substantial decreases in Arg and Val were observed, indicating that the changes in amino acid profiles varied depending on the bacterial strain and culture medium composition (Table 7). In this sense, the impact of fermentation on amino acid metabolism is sample-specific, with distinct differences observed between amino acid formation and consumption. This indicates that amino acid metabolism during fermentation varies depending on the medium used and the microorganisms involved. Peng et al. [46] explained the decrease in amino acids because of their conversion, via LAB metabolism, into aldehydes, carboxylic acids, and/or alcohols, while attributing the increase to the breakdown of cellular proteins or the interconversion of amino acids mediated by bacterial enzymes. Also, ESM, a significant biological waste product, consists of collagen-like proteins and glycosaminoglycans (GAGs), such as hyaluronic acid (HA). Lien et al. [47] found high levels of the amino acids Gly and Ser in hydrolysates derived from ESM. An assessment of the overall amino acid composition revealed that acid hydrolysis yielded 34.7% essential amino acids, while hydrolysis using keratinase yielded 35.4% essential amino acids.

The amino acids present in peptides can be classified by various characteristics, including essential/non-essential, polar/nonpolar, hydrophobic/hydrophilic, acidic/basic, and aromatic/aliphatic. The functional diversity of peptides is influenced by their amino acid composition and sequence [48]. Protein hydrolysates and antimicrobial peptides derived from food by-products, characterized by high levels of hydrophobic and basic amino acids, can offer benefits not only in nutrition but also in functionality and bioactivity [49].

When amino acid groups are evaluated collectively, the effect of 24-h fermentation varies by sample and amino acid group (Table 8, $p < 0.01$). By the end of the fermentation period, total amino acid (TAA) levels increased in the CLA, ELA, ELC, and ELR samples, while they decreased in the CLC and CLR samples. Notably, the ELA sample reached a higher TAA level at 24 h compared to the other samples. Throughout the fermentation process, the levels of essential amino acids (EAAs)—leucine, isoleucine, valine, methionine, phenylalanine, lysine, histidine, tryptophan, and threonine—increased in all samples except those containing *L. rhamnosus*. At the end of the fermentation, the highest levels of non-essential amino acids (NEAAs)—arginine, alanine, serine, glycine, proline, tyrosine, aspartic acid, glutamic acid, cysteine, and GABA—were observed in the ELR sample ($p < 0.01$). Warakaulle et al. [50] noted that variations in the amino acid sequences of casein proteins, combined with the metabolic activity of the selected bacterial strains, influence amino acid levels following fermentation. The most significant change regarding basic amino acids (BAAs)—arginine, histidine, lysine—was also observed in the ELA sample, which showed higher levels at 24 h than the other samples ($p < 0.01$). While an increase was also observed in the ELC sample, decreases were observed in the CLA, CLC, CLR, and ELR samples. The higher BAA value in the ELA sample can be attributed to the elevated levels of His, Arg, and Lys, as indicated in the preceding table of individual amino acids. The amounts of hydrophobic amino acids (HBAAs)—proline, alanine, valine, threonine, glycine, phenylalanine, leucine, and isoleucine—increased by the end of fermentation in CLA, CLC, and ELC samples, whereas they decreased in CLR, ELA, and ELR samples. By the end of fermentation, the ELC sample reached the highest HBAA level ($p < 0.01$). The levels of hydrophilic amino acids (HLAAs)—lysine, serine, arginine, aspartic acid, and glutamic acid—generally showed a downward trend by the end of fermentation. While

decreases relative to initial values were observed in CLA, CLC, CLR, ELC, and ELR samples, the change in the ELA sample was more limited. This may be attributed to the utilization of the released hydrophilic amino acids during bacterial growth and metabolic activities, or their conversion into other metabolites.

The levels of aromatic amino acids (AAAs), including tyrosine, phenylalanine, and tryptophan, showed notable changes during fermentation, increasing in all samples except CLR, where a decrease was observed (Table 8). At the end of fermentation, the ELR sample exhibited the highest AAA content ($p < 0.01$). As shown in Table 8, the high concentration of tyrosine (Tyr) in this sample indicates that the elevated AAA value in the ELR sample is largely attributable to tyrosine. Therefore, it is more accurate to interpret the AAA results not merely as a general indicator of proteolysis, but specifically in the context of tyrosine accumulation. Sulfur-containing amino acids (SAAs), cysteine and methionine, showed more limited variation compared to other amino acid groups. ELA sample increased, whereas CLA, CLR, ELC, and ELR samples decreased; no significant difference was observed for the CLC sample. The fact that ESM contains proteins rich in cysteine is particularly relevant to this group. Aromatic amino acids serve as important substrates in the metabolism of LAB; specifically, phenylalanine, tyrosine, and tryptophan can be converted into microbial metabolites such as phenyllactic acid, 4-hydroxyphenyllactic acid, and indole-3-lactic acid, respectively. Furthermore, these metabolic conversions may vary with the specific microorganism used and the fermentation conditions [51].

Regarding acidic amino acids (ACAAs)—aspartic and glutamic acids—a distinct profile emerged across the different groups. An increase was observed in the ELA and CLA samples (which contain *L. acidophilus*), while a decrease was noted in the other samples. The levels of polar amino acids (PAAs)—including cysteine, methionine, serine, threonine, and tyrosine—increased after fermentation in all samples except CLR, which showed a slight decrease (Table 8). Notably, the ELA, ELC, and ELR samples—which were supplemented with ESM—exhibited high PAA levels post-fermentation; in fact, all three ESM-containing samples stood out for their polar amino acid content. A different trend was observed for nonpolar amino acids (NPAAs)—including glycine, alanine, valine, isoleucine, leucine, proline, methionine, tryptophan, and phenylalanine—compared to the other amino acid groups. While higher levels were detected in the CLA and CLC samples after fermentation, decreases were observed in the CLR, ELA, ELC, and ELR samples.

3.5. Determination of Lactic Acid and Short-Chain Fatty Acids (SCFAs)

The levels of lactic acid and short-chain fatty acids (acetic, butyric, and propionic), metabolites produced by bacteria, were measured over a 24-h fermentation period (Table 9). While lactic acid concentrations increased significantly ($p < 0.01$) in all control groups (CLA, CLC, and CLR) by the end of the 24-h fermentation, the groups containing eggshell (ELA, ELC, and ELR) showed varied results, depending on the specific microorganism and its corresponding fermentation kinetics. The highest lactic acid concentration at the end of the fermentation was observed in the CLR (3082.88 mg/kg). In the CLC group, the initially high concentrations of acetic, butyric, and propionic acids decreased after 24 h of fermentation. In LAB, pyruvate metabolism can lead to the formation of various end products, such as lactate and acetate, depending on environmental conditions and substrate availability [52]. However, given that the formation of propionate and butyrate is closely linked to distinct microbial metabolic pathways, it is difficult to attribute the initial concentrations observed in the CLC group solely to the metabolism of *L. casei*. This suggests that the metabolite composition of the initial medium or components derived from the inoculum may have contributed to the organic acid profile.

Table 9. Changes in lactic acid and SCFA values of the samples (mg/kg).

Samples	FT	Lactic Acid	Acetic Acid	Butyric Acid	Propionic Acid
CLA	0	1217.31 ± 14.610 ^{aB}	4674.95 ± 70.100 ^{cB}	869.02 ± 15.640 ^{dB}	228.88 ± 4.810 ^{cB}
	24	2249.90 ± 33.700 ^{bA}	7741.33 ± 139.300 ^{aA}	3587.71 ± 75.300 ^{aA}	1660.26 ± 19.900 ^{aA}
CLC	0	855.54 ± 15.400 ^{cB}	66322.08 ± 1393 ^{aA}	46479.30 ± 558 ^{aA}	34377.30 ± 516 ^{aA}
	24	1402.40 ± 29.500 ^{cA}	1405.90 ± 16.870 ^{eB}	1154.29 ± 17.300 ^{cB}	252.75 ± 4.550 ^{eB}
CLR	0	1131.27 ± 13.570 ^{bB}	4482.05 ± 67.200 ^{cA}	834.58 ± 15.020 ^{dA}	458.34 ± 9.630 ^{cA}
	24	3082.88 ± 46.200 ^{aA}	3380.13 ± 69.800 ^{cB}	837.60 ± 17.600 ^{dA}	286.55 ± 3.440 ^{dB}
ELA	0	814.35 ± 14.660 ^{dA}	5103.04 ± 107.200 ^{cA}	1721.83 ± 20.700 ^{cA}	1328.98 ± 19.900 ^{bA}
	24	315.02 ± 6.610 ^{eB}	1282.83 ± 15.390 ^{eB}	721.67 ± 10.820 ^{eB}	383.61 ± 6.900 ^{cB}
ELC	0	315.61 ± 3.790 ^{eB}	17707.69 ± 266 ^{bA}	2452.92 ± 44.200 ^{bA}	1425.45 ± 29.900 ^{bA}
	24	616.74 ± 9.250 ^{dA}	3930.32 ± 70.700 ^{bB}	1652.56 ± 34.700 ^{bB}	816.66 ± 9.800 ^{bB}
ELR	0	646.08 ± 11.630 ^{eA}	3113.93 ± 64.400 ^{dA}	766.11 ± 9.190 ^{dA}	456.57 ± 6.850 ^{cA}
	24	313.80 ± 6.690 ^{eB}	1993.70 ± 23.900 ^{dB}	597.04 ± 8.960 ^{fB}	254.63 ± 4.580 ^{eB}

Note: Different lowercase superscript letters represent significant differences ($p < 0.01$) among media, whereas different uppercase superscript letters represent significant differences ($p < 0.01$) between the fermentation times. CLA: culture medium containing *L. acidophilus*; CLC: culture medium containing *L. casei*; CLR: culture medium containing *L. rhamnosus*; ELA: culture medium containing eggshell membrane protein and *L. acidophilus*; ELC: culture medium containing eggshell membrane protein and *L. casei*; ELR: culture medium containing eggshell membrane protein and *L. rhamnosus*; FT: fermentation time.

In the CLA sample, the concentrations of lactic and acetic acids increased by the end of the fermentation process; in contrast, the ELA sample, which used the same microorganism but included eggshell, showed decreases in both acids. This suggests that the composition of the growth medium can influence the organic acid profile. The relationships among microbial growth, amino acid composition, and organic acid production further highlight the strain-dependent effects of culture medium composition. In the ESM-containing *L. acidophilus* medium (ELA), the higher total amino acid concentration was accompanied by a lower maximum specific growth rate and lower lactic acid concentration than in the corresponding control (CLA). This suggests that amino acid accumulation does not necessarily correspond to enhanced bacterial growth or acid production, as nutrient utilization also depends on substrate accessibility and strain-specific metabolic requirements. In contrast, *L. casei* exhibited an increased growth rate in the ESM-containing medium, indicating a different response to the modified nutrient composition. Although glucose was maintained at the same concentration, replacing conventional complex nitrogen sources with ESM may have influenced the balance between bacterial growth, amino acid metabolism, and organic acid production. One possible mechanism for these observed differences is that $CaCO_3$, the primary component of eggshells, may neutralize acids within the fermentation environment, thereby affecting the pH balance. Nevertheless, further monitoring of the fermentation process is required to determine whether the lower short-chain fatty acid concentrations in the ELA group result directly from $CaCO_3$ neutralization or from changes in microbial metabolism. These findings indicate that the lactic and short-chain fatty acid profile emerging during fermentation can vary with the composition of the medium and the type of microorganism involved.

4. Conclusions

This study demonstrated that the effects of eggshell membrane (ESM) protein on the growth kinetics and metabolite profiles of probiotic *lactobacilli* were strain-dependent. ESM-containing media increased the maximum specific growth rate and estimated maximum cell counts of *L. casei*, whereas *L. acidophilus* and *L. rhamnosus* exhibited lower growth rates and longer adaptation periods. Significant changes in amino acid profiles, particularly increased total amino acid content in *L. acidophilus*, were observed, while lactic acid and short-chain fatty acid concentrations varied among strains and culture media. Among the predictive approaches, Gaussian process regression (GPR) achieved the lowest mean cross-validated prediction error (CV_RMSE = 0.1344 $\log_{10}$ CFU/mL), although the best-performing model varied across culture conditions.

These findings highlight the potential of ESM as an alternative medium component for strain-specific probiotic fermentation. However, differences in nitrogen sources between the control and ESM-containing media, the lack of direct investigation of metabolic mechanisms, and the limited validation of predictive models should be considered. Future studies should focus on optimizing ESM concentrations, elucidating strain-specific metabolic responses, validating growth models under independent fermentation conditions, and evaluating the feasibility of ESM-based media through pilot-scale fermentation studies.

Author Contributions: Conceptualization, T.O.; methodology, T.O. and G.K.; software, M.O.O.; validation, M.O.O.; formal analysis, T.O., L.Y.-E., G.K., M.B.N. and M.O.O.; investigation, T.O., L.Y.-E., G.K., M.B.N. and M.O.O.; resources, T.O.; data curation, T.O., L.Y.-E., G.K., M.B.N. and M.O.O.; writing—original draft preparation, T.O., L.Y.-E., G.K., M.B.N. and M.O.O.; writing—review and editing, T.O., L.Y.-E., G.K., M.B.N. and M.O.O.; project administration, T.O. All authors have read and agreed to the published version of the manuscript.

Funding: This research was funded by the Scientific Research Projects Coordination Unit of Bursa Uludag University (grant number: FGA-2025-2421).

Institutional Review Board Statement: Not applicable.

Informed Consent Statement: Not applicable.

Data Availability Statement: The original contributions in this study are included in the article. Further inquiries can be directed to the corresponding author.

Acknowledgments: During the preparation of this manuscript, the authors used OpenAI to assist with drafting and language editing. The authors have reviewed and edited the generated content and take full responsibility for the final manuscript.

Conflicts of Interest: The authors declare no conflicts of interest.

Abbreviations

The following abbreviations are used in this manuscript:

AAA	Aromatic Amino Acid
ACAA	Acidic Amino Acid
ANOVA	Analysis of Variance
BAA	Basic Amino Acids
CV_MAE	Cross-Validated Mean Absolute Error
CV_R^2	Cross-Validated Coefficient of Determination
CV_RMSE	Cross-Validated Root Mean Squared Error
DAD	Diode Array Detector
EAA	Essential Amino Acid
ESM	Eggshell Membrane
GABA	Gamma-Aminobutyric Acid

GPR	Gaussian Process Regression
HBAA	Hydrophobic Amino Acid
HLAA	Hydrophilic Amino Acid
HPLC	High-Performance Liquid Chromatography
LAB	Lactic Acid Bacteria
LSD	Least Significant Difference
MRS	de Man, Rogosa and Sharpe
NEAA	Non-Essential Amino Acid
NPAA	Nonpolar Amino Acid
PAA	Polar Amino Acid
R^2	Coefficient of Determination
RMSE	Root Mean Squared Error
SAA	Sulfur-Containing Amino Acid
SCFA	Short-Chain Fatty Acid
SD	Standard Deviation
SSE	Sum of Squared Errors
SVR	Support Vector Regression
TAA	Total Amino Acid

References

1. Anonymous. Food and Agriculture Organization of the United Nations Official Website. Available online: https://www.fao.org/faostat/en/#compare (accessed on 16 September 2026).
2. Park, S.; Choi, K.S.; Lee, D.; Kim, D.; Lim, K.T.; Lee, K.H.; Hoon, S.W.; Kim, J. Eggshell membrane: Review and impact on engineering. *Biosyst. Eng.* **2016**, *151*, 446–463. [CrossRef]
3. Yuceer, M. Value-added from waste: Eggshell membrane. *J. Cent. Union Egg Prod.* **2021**, *55*, 42–45.
4. Liang, X.; Cong, H.; Jiang, G.; He, H. Enhancing physicochemical and piezoelectric properties of eggshell membrane proteins by ultrasonic-assisted enzymes for food and sensor applications. *Int. J. Mol. Sci.* **2025**, *26*, 2190. [CrossRef] [PubMed]
5. Taylor, R.C.; Omed, H.; Edwards-Jones, G. The greenhouse emissions footprint of free-range eggs. *Poult. Sci.* **2014**, *93*, 231–237. [CrossRef] [PubMed]
6. Iftikhar, L.; Ahmad, I.; Saleem, M.; Rasheed, A.; Waseem, A. Exploring the chemistry of waste eggshells and its diverse applications. *Waste Manag.* **2024**, *189*, 348–363. [CrossRef] [PubMed]
7. Xiao, N.; Huang, X.; He, W.; Yao, Y.; Wu, N.; Xu, M.; Du, H.; Zhao, Y.; Tu, Y. A review on recent advances of egg byproducts: Preparation, functional properties, biological activities and food applications. *Food Res. Int.* **2021**, *147*, 110563. [CrossRef] [PubMed]
8. Liang, X.; Cong, H.; Jiang, G.; Rao, R.P.; He, H.; Ramakrishna, S. Eggshell membrane: Structure, purification, properties and multifunctional applications. *Food Biosci.* **2024**, *60*, 104487. [CrossRef]
9. Han, C.; Chen, Y.; Shi, L.; Chen, H.; Li, L.; Ning, Z.; Zeng, D.; Wang, D. Advances in eggshell membrane separation and solubilization technologies. *Front. Vet. Sci.* **2023**, *10*, 1116126. [CrossRef] [PubMed]
10. Warman, D.J.; Jia, H.; Hasebe, Y.; Kato, H. Eggshell membrane, a resistant protein, possesses prebiotic-like properties in improving gut microbiota composition and gut-liver axes in chronologically aged C57BL/6J male mice. *J. Funct. Foods* **2024**, *123*, 106610. [CrossRef]
11. Ramli, N.S.; Jia, H.; Sekine, A.; Lyu, W.; Furukawa, K.; Saito, K.; Hasebe, Y.; Kato, H. Eggshell membrane powder lowers plasma triglyceride and liver total cholesterol by modulating gut microbiota and accelerating lipid metabolism in high-fat diet-fed mice. *Food Sci. Nutr.* **2020**, *8*, 2512–2523. [CrossRef] [PubMed]
12. Jain, S.; Anal, A.K. Production and characterization of functional properties of protein hydrolysates from egg shell membranes by lactic acid bacteria fermentation. *J. Food Sci. Technol.* **2017**, *54*, 1062–1072. [CrossRef] [PubMed]
13. Mudawaroch, R.E.; Setiyono, S.; Yusiati, L.M.; Suryanto, E. Fermentation kinetics of isolate lactic acid bacteria probiotic BR 12 and BR 17 were isolated from broiler chicken meat. In *Proceedings of the International Conference on Environmental Awareness for Sustainable Development in Conjunction with International Conference on Challenge and Opportunities Sustainable Environmental Development (ICEASD & ICCOSED 2019), Kendari, Indonesia, 1–2 April 2019*; European Alliance for Innovation: Bratislava, Slovakia, 2019. [CrossRef]
14. Keser, G.; Ozcan, T. Cross-over fermentation dynamics and proteomic properties of acid gels with indigenous *Lactobacillus* spp. isolated from cheeses. *Food Microbiol.* **2025**, *128*, 104700. [CrossRef] [PubMed]

15. Lo Grasso, A.; Fort, A.; Mahdizadeh, F.F.; Magnani, A.; Mocenni, C. Generalized logistic model of bacterial growth. *Math. Comput. Model. Dyn. Syst.* **2023**, *29*, 169–185. [CrossRef]
16. Sharma, V.; Mishra, H.N. Unstructured kinetic modeling of growth and lactic acid production by *Lactobacillus plantarum* NCDC 414 during fermentation of vegetable juices. *LWT Food Sci. Technol.* **2014**, *59*, 1123–1128. [CrossRef]
17. Lee, S.; Lee, H.; Kim, S.; Lee, J.; Ha, J.; Gwak, E.; Oh, M.-H.; Park, B.-Y.; Kim, J.-S.; Choi, K.-H.; et al. Probabilistic models to describe the effect of $NaNO_2$ in combination with NaCl on the growth inhibition of *Lactobacillus* in frankfurters. *Meat Sci.* **2015**, *110*, 302–309. [CrossRef] [PubMed]
18. Swain, P.S.; Stevenson, K.; Leary, A.; Montano-Gutierrez, L.F.; Clark, I.B.N.; Vogel, J.; Pilizota, T. Inferring time derivatives including cell growth rates using Gaussian processes. *Nat. Commun.* **2016**, *7*, 13766. [CrossRef] [PubMed]
19. Smola, A.J.; Schölkopf, B. A tutorial on support vector regression. *Stat. Comput.* **2004**, *14*, 199–222. [CrossRef]
20. Ozcan, T.; Keser, G.; Kaya, A.R.; Cetin, Y.E.; Elciboga, F. Modulation of biofunctional and structural properties in stevia-sweetened ice cream by lactic fermentation. *Food Sci. Nutr.* **2026**, *14*, e72030. [CrossRef] [PubMed]
21. Ashraf, R.; Smith, S.C. Selective enumeration of dairy based strains of probiotic and lactic acid bacteria. *Int. Food Res. J.* **2015**, *22*, 2576–2586.
22. Narli, M.B.; Ozcan, T. Assessment of bifidogenic potential of cowpea (*Vigna unguiculata* (L.) Walp.) extract in *in vitro* and milk fermentation models. *LWT* **2022**, *157*, 113071. [CrossRef]
23. Zwietering, M.H.; Jongenburger, I.; Rombouts, F.M.; van't Riet, K. Modeling of the bacterial growth curve. *Appl. Environ. Microbiol.* **1990**, *56*, 1875–1881. [CrossRef] [PubMed]
24. Baranyi, J.; Roberts, T.A. A dynamic approach to predicting bacterial growth in food. *Int. J. Food Microbiol.* **1994**, *23*, 277–294. [CrossRef] [PubMed]
25. Pedregosa, F.; Varoquaux, G.; Gramfort, A.; Michel, V.; Thirion, B.; Grisel, O.; Blondel, M.; Prettenhofer, P.; Weiss, R.; Dubourg, V.; et al. Scikit-learn: Machine learning in Python. *J. Mach. Learn. Res.* **2011**, *12*, 2825–2830.
26. Adin, A.; Krainski, E.T.; Lenzi, A.; Liu, Z.; Martínez-Minaya, J.; Rue, H. Automatic cross-validation in structured models: Is it time to leave out leave-one-out? *Spat. Stat.* **2024**, *62*, 100843. [CrossRef]
27. Kose, S.; Kaklıkkaya, N.; Koral, S.; Tufan, B.; Buruk, K.C.; Aydın, F. Commercial test kits and the determination of histamine in traditional (ethnic) fish products-evaluation against an EU accepted HPLC method. *Food Chem.* **2011**, *125*, 1490–1497. [CrossRef]
28. Aktas, A.H.; Sen, S.; Yilmazer, M.; Cubuk, E. Determination of carboxylic acids in apple juice by RP HPLC. *Iran. J. Chem. Chem. Eng.* **2005**, *24*, 1–6. [CrossRef]
29. Yilmazer, M.; Secilmis, H. Analysis of some dairy-ındependent aroma components by gas chromatography headspace system. In Proceedings of the 9th Turkish Food Congress, Bolu, Türkiye, 24–26 May 2006.
30. Bisson, G.; Marino, M.; Poletti, D.; Innocente, N.; Maifreni, M. Turbidimetric definition of growth limits in probiotic *Lactobacillus* strains from the perspective of an adaptation strategy. *J. Dairy Sci.* **2021**, *104*, 12236–12248. [CrossRef] [PubMed]
31. Slizewska, K.; Chlebicz-Wojcik, A. Growth kinetics of probiotic *Lactobacillus* strains in the alternative, cost-efficient semi-solid fermentation medium. *Biology* **2020**, *9*, 423. [CrossRef] [PubMed]
32. Savijoki, K.; Ingmer, H.; Varmanen, P. Proteolytic systems of lactic acid bacteria. *Appl. Microbiol. Biotechnol.* **2006**, *71*, 394–406. [CrossRef] [PubMed]
33. Khalfallah, R.; Mechmeche, M.; Jmoui, I.; Ksontini, H.; Hamdi, M.; Kachouri, F. Growth kinetics of *Lactobacillus plantarum* in sesame seed protein extract media. *Chem. Afr.* **2023**, *6*, 1217–1226. [CrossRef]
34. Shi, Y.; Zhou, K.; Li, D.; Guyonnet, V.; Hincke, M.T.; Mine, Y. Avian eggshell membrane as a novel biomaterial: A review. *Foods* **2021**, *10*, 2178. [CrossRef] [PubMed]
35. Liu, M.; Bayjanov, J.R.; Renckens, B.; Nauta, A.; Siezen, R.J. The proteolytic system of lactic acid bacteria revisited: A genomic comparison. *BMC Genom.* **2010**, *11*, 36. [CrossRef] [PubMed]
36. Zhu, L.; Li, J.; Guyonnet, V.; Xu, Y.; Dai, Q.; Zhang, M.; Wang, H.; Yi, Y.; Xu, W. Unveiling dual-functional umami peptides with antioxidant effects from eggshell membrane byproducts: A machine learning-guided approach integrating molecular simulation and quantum chemistry. *Food Chem. X* **2025**, *32*, 103343. [CrossRef] [PubMed]
37. Sun, J.; Lv, X.; Zhang, M.; Xu, B. Eggshell membrane peptides: From preparation and flavor modulation to Nano-delivery systems. *Food Chem.* **2026**, *527*, 150849. [CrossRef] [PubMed]
38. Bintsis, T. Lactic acid bacteria as starter cultures: An update in their metabolism and genetics. *AIMS Microbiol.* **2018**, *4*, 665. [CrossRef] [PubMed]
39. Bergamini, C.V.; Hynes, E.R.; Candioti, M.C.; Zalazar, C.A. Multivariate analysis of proteolysis patterns differentiated the impact of six strains of probiotic bacteria on a semi-hard cheese. *J. Dairy Sci.* **2009**, *92*, 2455–2467. [CrossRef] [PubMed]
40. Zhu, L.; Ma, M.; Ahn, D.U.; Guyonnet, V.; Wang, L.; Zheng, Y.; He, Q.; Xiong, H.; Huang, X. Hatched eggshell membrane can be a novel source of antioxidant hydrolysates to protect against H_2O_2-induced oxidative stress in human chondrocytes. *Antioxidants* **2022**, *11*, 2428. [CrossRef] [PubMed]

41. Papadimitriou, K.; Alegría, Á.; Bron, P.A.; De Angelis, M.; Gobbetti, M.; Kleerebezem, M.; Lemos, J.A.; Linares, D.M.; Ross, P.; Stanton, C.; et al. Stress physiology of lactic acid bacteria. *Microbiol. Mol. Biol. Rev.* **2016**, *80*, 837–890. [CrossRef] [PubMed]
42. Lv, X.; Liu, G.; Sun, X.; Chen, H.; Sun, J.; Feng, Z. Nutrient consumption patterns of *Lactobacillus acidophilus* KLDS 1.0738 in controlled pH batch fermentations. *J. Dairy Sci.* **2017**, *100*, 5188–5194. [CrossRef] [PubMed]
43. Hwang, H.; Lee, J.H. Characterization of arginine catabolism by lactic acid bacteria isolated from kimchi. *Molecules* **2018**, *23*, 3049. [CrossRef] [PubMed]
44. Jung, S.; Chang, J.Y.; Lee, J.H. Arginine metabolism and the role of arginine deiminase-producing microorganisms in kimchi fermentation. *Heliyon* **2022**, *8*. [CrossRef] [PubMed]
45. Kieliszek, M.; Pobiega, K.; Piwowarek, K.; Kot, A.M. Characteristics of the proteolytic enzymes produced by lactic acid bacteria. *Molecules* **2021**, *26*, 1858. [CrossRef] [PubMed]
46. Peng, S.; Yang, L.; Zhou, W.; Yuan, Y.; Liao, L.; Huang, X.; Zhang, C.; Gong, X.; Li, J. Effects of *Lacticaseibacillus casei* LK-1 fermentation on physicochemical properties, chemical compositions, antioxidant activities and volatile profiles of pineapple juice. *Foods* **2025**, *14*, 3474. [CrossRef] [PubMed]
47. Lien, Y.C.; Lai, S.J.; Lin, C.Y.; Wong, K.P.; Chang, M.S.; Wu, S.H. High-efficiency decomposition of eggshell membrane by a keratinase from *Meiothermus taiwanensis*. *Sci. Rep.* **2022**, *12*, 14684. [CrossRef] [PubMed]
48. Jiang, Y.; Sun, J.; Chandrapala, J.; Majzoobi, M.; Brennan, C.; Zeng, X.A.; Sun, B. Recent progress of food-derived bioactive peptides: Extraction, purification, function, and encapsulation. *Food Front.* **2024**, *5*, 1240–1264. [CrossRef]
49. Davoudi, M.; Gavlighi, H.A.; Javanmardi, F.; Benjakul, S.; Nikoo, M. Antimicrobial peptides derived from food byproducts: Sources, production, purification, applications, and challenges. *Compr. Rev. Food Sci. Food Saf.* **2024**, *23*, e13422. [CrossRef] [PubMed]
50. Warakaulle, S.; Ayyash, M.M.; Kamal-Eldin, A. Profiling protein hydrolysis and amino acid metabolism in camel and bovine milk fermented by *Lactobacillus helveticus*, *L. bulgaricus*, and *Streptococcus thermophilus*. *Sci. Rep.* **2025**, *15*, 18371. [CrossRef] [PubMed]
51. Kasperek, M.C.; Galeas, A.V.; Caetano-Silva, M.E.; Xie, Z.; Ulanov, A.; La Frano, M.; Devkota, S.; Miller, M.J.; Allen, J.M. Microbial aromatic amino acid metabolism is modifiable in fermented food matrices to promote bioactivity. *Food Chem.* **2024**, *454*, 139798. [CrossRef] [PubMed]
52. Gänzle, M.G. Lactic metabolism revisited: Metabolism of lactic acid bacteria in food fermentations and food spoilage. *Curr. Opin. Food Sci.* **2015**, *2*, 106–117. [CrossRef]

Disclaimer/Publisher's Note: The statements, opinions and data contained in all publications are solely those of the individual author(s) and contributor(s) and not of MDPI and/or the editor(s). MDPI and/or the editor(s) disclaim responsibility for any injury to people or property resulting from any ideas, methods, instructions or products referred to in the content.